CHAPTER **3**

INTERPRETATION, APPRAISAL, AND APPLICATION

INTERPRETATION

The primary reason for initiating this study was to develop guidelines and computational vehicles for designing laterally loaded groups of piles for transportation structures. The emphasis was on extreme-event dynamic loading, such as ship impact and seismic loading. As the research developed, it appeared that this type of loading would be amenable to analysis by means that have been well developed in the past for modeling the static behavior of laterally loaded pile groups. That is, by applying inertial effects to the structural elements; using static stiffness relationships for the soil (in the form of *p-y* curves); adding soil damping through either a viscous damping factor or hysteresis and gapping in the *p-y* model; using *p*-multipliers developed from previous, full-scale and centrifuge static load testing; and employing minor structural material damping, solutions to inertial loading events (i.e., loading through the pile cap) could be obtained that are sufficiently accurate for design purposes.

A computational model, a dynamic version of FLPIER, was developed to include the characteristics listed above. This model was then verified against a series of full-scale static and impulse-type dynamic tests performed in the field at two sites. The impulse loading events used in the field tests can be classified as "inertial," in the sense that loading was applied through the cap, rather than "kinematic," in which the loading would be applied to the piles to the soil. Seismic loading is a combination of inertial and kinematic loading. Although FLPIER was not verified for the case of loading through the soil, it was programmed with the capability to model such loading through time-domain motion of the supports for the *p-y* curves; the motion mimics free-field ground motion.

Although it should be possible to include a liquefaction model in the *p-y* curve formulation, in neither the field tests nor FLPIER was any attempt made to model explicitly the effects of liquefying soil.

This approach to modeling the test groups appeared to give results that are sufficiently accurate for the design of pile groups in nonliquefying soils at a limited number of sites and generally should be applicable to the design of pile groups in nonliquefying soil as the number of sites at which the method has been calibrated increases. It should be pointed out that this approach is not limited to the code used here (i.e., FLPIER), but should apply to any structural program that includes the inertia of structural elements and uses hysteretic *p-y* curves that can be modified by *p*-multipliers.

APPRAISAL

Using the general inputs described above and without using viscous damping factors for the soil, the computational tool FLPIER(D) provided reasonable predictions of the field test behavior, with two exceptions. First, the program did not give reasonable results when the pile heads were specified to be partially fixed (i.e., rotation permitted with some resisting moment developing) to the pile cap. Second, the program did not predict accurately the distribution of either head shears or bending moments among the various piles. The first deficiency likely is due to a "bug" in the program that has not yet been located. In due time, it is expected that this problem will be solved, but it could not be solved in the time frame available to the research team. The second deficiency appears not to be a deficiency in the program, but rather to be a result of spatial variations in lateral soil resistance among the locations of the individual piles in the group that is not associated with group action. For example, it was shown that extreme differences in the installation method (e.g., boring and casting piles in place versus driving displacement piles) produced rather large differences in soil resistance against both individual piles and pile groups at an independent test site in Taiwan. For this reason, it is recommended that the ideal (computed) maximum shears and moments in the various piles be multiplied by a load factor before the piles are designed structurally.

The field test program included only two sites that, although dissimilar, did not represent geotechnically all of the soil types of concern in designing laterally loaded pile groups for extreme events. When using the approach described here, it is expected that the most accurate designs for impact or seismic loading will be achieved when full-scale pile group tests are tested at the site of interest. In the event that large, portable inertial vibrators become available in the future, using vibrators instead of the Statnamic device will undoubtedly prove more appropriate for simulating seismic loading. The test piles that were developed for this project would be appropriate for future field studies; however, the steel frame should be abandoned in favor of using a cast-in-place concrete cap.

APPLICATION

The results and analyses of the field load test program suggest the following engineering guidelines for the design of pile groups subject to lateral loading.

Pile-Soil-Pile Interaction and Group Effects

The use of *p*-multipliers derived from static testing, as implemented in FLPIER, is an effective means of modeling the effects of group action on the soil resistance. In granular soils, consideration should be given to reducing the default values of the *p*-multipliers (see Table 3) when bored piles (i.e., drilled shafts) are used by (1) about 40 percent on the leading row if row-by row *p*-multipliers are used or (2) about 20 percent if a single, average *p*-multiplier is used for all rows of piles. The default values provided in FLPIER (see Table 3) from the soils at the field test sites for 3D and 4D c-c pile spacing appeared appropriate when the piles were driven displacement piles. For the rare case in which closer spacings (2.5D) are used and granular soil is present near the ground surface, the *p*-multipliers that are approximated from Figure 9 are recommended for use.

Although the general trend of distribution of shear and moment to the piles within a group is similar by row position to the trend predicted by the row position–based *p*-multipliers in Table 3, the actual distribution of shear and moment that might be expected among the piles in the row considered on a realistic, full-sized pile group foundation is subject to significant random variations because of variations in soil properties. This unpredictable variability is at least as significant as any geometric variability; therefore, designers should provide accommodations for variability of computed maximum bending moments in the piles by multiplying the computed average maximum moment for a pile in a given row by a load (i.e., moment multiplication) factor of about 1.2 before completing the structural design of the piles.

The use of a simple average *p*-multiplier for all piles in the group based on a computed weighted average of the individual piles based on row position provides a computed response that is equally suitable for design purposes. Given the uncertainties related to the above-noted variability and to the unknown, reversible, and likely variable direction of loading from a seismic event, it appears sufficient for design purposes to use this simplified approach.

The test data and the modeling efforts both indicate strong coupling between lateral and rotational stiffness. The axial pile stiffness has a major influence on the rotation of the cap, and this stiffness is strongly coupled to the lateral stiffness. The use of group models such as FLPIER or other computer codes that include axial stiffness of the piles are recommended. The use of uncoupled analyses could significantly underestimate or overestimate the lateral stiffness, particularly if the pile cap is assumed not to rotate.

Dynamic Behavior

The lateral dynamic response for large lateral loads that are similar to extreme-event loading is strongly nonlinear, even when the structural response of the piles and cap is within the linear elastic range. The damped resonant frequency is reduced and the damping increases with increasing displacement amplitudes; therefore, damping needs to be included in the design model (e.g., FLPIER).

If funds are available at a bridge site, Statnamic loading of a test group should be strongly considered, especially in the case of critical structures. The Statnamic loading device provides a mechanism to apply large lateral loads to a test foundation with a force time history that is close to the resonant frequency of a full-scale test foundation. Except for the largest pile groups, this system is effective at inducing large-amplitude dynamic motions in test foundations and provides a means of obtaining meaningful dynamic measurements of the system response. The Statnamic loading mechanism is limited in producing the cyclic degradation in soil strength and stiffness that might be expected during a seismic or repeated loading event and could be replaced with a portable vibrator. At present, however, inertial vibrators with force amplitudes large enough to produce lateral deformations in the piles equivalent to those that are expected in major seismic events in full-scale pile groups are not available. When the vibrators become available, they may be employed in place of the Statnamic device.

A simple SDOF model for evaluating the dynamic response of a pile group to Statnamic impulse loading, however, can be very useful for identifying fundamental system properties and extracting nonlinear static stiffness, which is the most important parameter in predicting dynamic response. SDOF modeling can be done independently of computer simulations and may, in certain circumstances, be sufficient for evaluating the response of the pile group.

For more in-depth analysis, FLPIER(D) or a similar code should be used to simulate the behavior of the group. Modeling the dynamic response of the soil using hysteretic, static *p-y* curves and static *p*-multipliers seems to capture well the most important aspects of foundation behavior during dynamic loading. The inertial effects of the structure above grade are straightforward and must be included in the simulation because they are important to the overall system response. Some small amount of system damping, which can be modeled with additional participating mass, may be considered, but this damping does not appear to be a major influence on the foundation. Compared with the static response, the most important elements in the dynamic soil response are the gapping and hysteretic damping and the rate effects in cohesive soils. Radiation damping may contribute to overall damping, but it is difficult to separate the effects of radiation damping from that of hysteretic damping. For this reason, all damping for low-frequency, large-displacement (i.e., $y/D > 0.05$) loading is modeled as hysteretic for seismic loading conditions.

The static stiffness is the dominant component of resistance to lateral load for the low-frequency motion characteristic of a full-scale group of piles or shafts (in the range of 2 to 4 Hz). Damping adds significantly to the resistance at higher amplitudes of motion (e.g., in excess of 20 to 30 mm), with increasing effect at larger amplitudes. For vessel impact loads, which

may occur at a much lower rate of loading than seismic loading (e.g., load times on the order of several seconds to peak), the static response is likely to dominate most cases, and static analyses should be only slightly conservative (unless inertial components of the structure are substantial).

APPLICATION OF FLPIER(D) TO THE ANALYSIS AND DESIGN FOR SEISMIC LOADING

FLPIER(D), the dynamic version of FLPIER, was developed in this study to facilitate interpretation of the field test results and to serve as a design tool for those who wish to use it. It is emphasized that FLPIER(D) is one of many suitable tools that can be used to analyze pile groups under lateral loading.

The following is a summary of the process used to analyze a bridge pier for earthquake loading. This process assumes that the reader is familiar with FLPIER and how to develop models of bridge piers using the FLPier_Gen graphics generator. FLPier_Dyn_Gen is the equivalent generator in the new code, FLPIER(D). Some hand editing may be necessary because all of the capabilities for the FLPier_Dyn engine are not available in the FLPier_Dyn_Gen generator.

Before executing the program, users should download the program from www.ce.ufl.edu/nchrpdemo.html. A help file and a sample data file can be found on this download. This program will be disabled after December 31, 2001, as a precaution against propagating a new program that may have bugs. If the program has never been installed before, the user should understand that the graphics interface uses a font that most Windows 98 and new NT systems do not have. Users are encouraged to go to the software link at www.ce.ufl.edu/ and download the font for their operating system, following the instructions given at that site.

In order to illustrate the use of FLPIER(D), the following example is given. The analysis process is based on the results from the Statnamic field tests for this project and the ensuing dynamic model results using FLPIER(D).

Consider the following soil properties, which are assumed to apply to all of the piles at the location of the pier to be analyzed.

Example:

Layer	Thickness (in.)	Modulus (k/in.^{2})	Unit Weight (k/in.^{3})	Undrained Shear Strength (k/in.^{2})	ϵ_{50}	ϵ_{100}	Shear Modulus (k/in.^{2})	Poisson's Ratio	τ_f (k/in.^{2})	Tip Bearing Capacity (k/in.^{2})
1	360	0.5	0.000066	0.003	0.020	—	1.5	0.3	0.15	
2	480	0.5	0.000071	0.030	0.005	0.03	1.5	0.3	0.15	
Tip							1.5	0.3		0.27

NOTE: 1 k = 4.45 kN; 1 in. = 25.4 mm.

These properties were taken from soil borings near the subject pile group. The soil profile is similar to that at the Wilmington site (i.e., Cooper River Bridge) described earlier in this report and elaborated upon in Appendix D. From these data, an initial pile system was developed. Note that the parameter τ_f is the ultimate unit side resistance used by FLPIER or FLPIER(D) to produce axial unit load transfer curves. A very high value was used in this example analysis to force the response of the pile group to be translational in the lateral direction of loading, rather than both translational and rotational. In most cases, this value would be the estimated value of maximum unit side resistance.

The following step-by-step procedure is then followed to develop the input file.

Step 1: *Estimate an equivalent static load for initial sizing of the piles.*

Use 10 percent of the pier + bridge weight. For this example, 2,000 kips (8.9 MN) was used.

Step 2: *Create a pier model with a trial size and number of piles.*

The "Pseudo Dynamic Curve" option is used. This option requires an approximate fundamental period of the structure (17 cycles/s was chosen for this example) and the shear velocity of each soil layer. For this example, 2,000 in./s (50.8 m/s) was used for soil shear wave velocity.

Step 3: *Run this pseudo-dynamic option and iterate on the size and number of piles until the displacements of the pile head and the pile and pier moments are within design tolerance.*

Set the piles to "linear" with "properties," obtain convergence on the soil, change the pile to "nonlinear," and finalize the pile configuration. The file used for this analysis is included with the example files as part of the FLPier_Dyn install and is named "design_stdyn.in." (Note that the "nonlinear" option of the program automatically checks the moment capacity of the piles and pier elements because of the nonlinear bending. If the program converges, the pile sections have sufficient capacity.)

During the execution of this pseudo-dynamic phase of the analysis, FLPIER(D) used the following:

- The default *p-y* curves for the soil types encountered (Matlock soft-clay criteria [*42*] in Layer 1 and Reese et al. stiff-clay below-water-table criteria [*43*] in Layer 2).
- The simplified pseudo-dynamic reduction (i.e., damping) model in Appendix B for the *p-y* curves, which was turned on for the pseudo-static analysis (i.e., the preliminary sizing of the piles achieved in this phase). This model provides an estimate of damping and was assumed to apply to clay *p-y* curves (conditions in this case) as well as to sand *p-y* curves (conditions assumed in Appendix B). A different approach was used in the next phase, as described subsequently.
- A pile cap that was assumed to be flexible, but elastic. It was assigned a Young's modulus of 4,400 ksi (30.3 GPa).

Cap–soil interaction was not modeled. The piles were rigidly framed into the pile cap. (Note that at this time, only rigid framing and pinned connections should be assumed at the pile heads in FLPIER[D] because FLPIER[D] may have difficulty converging when partial pile-head fixity is specified.)

- The default *p*-multipliers. That is, values of 0.8, 0.4, 0.3, 0.2, and 0.3 were used from front row to back row in the 5-row × 4-column group that was finally developed. (Note that these would be appropriate for a driven pile group, but possibly not for a drilled shaft group in cohesionless sands below the water table, as is demonstrated in Appendix A. Because the shear wave velocity of the soft clay at this site is low, the natural frequency of the bridge is high, and the pile radii are large, a_o is very high [i.e., > 1]. Thus, the *p*-multipliers that are given for sand with value of a_o up to 0.12 in Figure B-41 and ahead in Figures B-42 and B-43 are not appropriate.)
- For axial loading, the maximum unit skin friction (t_f) and unit tip resistance are specified as shown in the example table on the previous page, and the default *t-z* curves in FLPIER for clay are applied automatically. No damping was assumed to occur because of axial loading of the piles as the cap rotates in response to a lateral load.

The pile group that was found to be satisfactory was a 5-row × 4-column group of steel pipe piles, each with a diameter of 60 in. (1.524 m), a wall thickness of 1.5 in. (38.1 mm), and a c-c spacing of 3D in both directions. A layout of this group is shown in Figure 42.

For that group, the final displacements given below were obtained. *X* is the displacement in the loading direction; *Y* is the transverse displacement; *Z* is the vertical displacement.

Summary of Displacements at Pile Heads Only

NODE	*X* (in.)	*Y* (in.)	*Z* (in.)
1	4.9487	–0.0001	–0.5371
2	4.9484	0.0001	–0.0060
3	4.9479	0.0002	0.5431
4	4.9487	0.0001	–0.5371
5	4.9484	–0.0001	–0.0060
6	4.9479	–0.0002	0.5431

NOTE: 1 in. = 25.4 mm.

Because the problem converged using the "nonlinear" option, the piles have sufficient capacity. The preliminary design has now been completed. The full time domain analysis using an actual or assumed earthquake record can be run next to provide a final check on the pile group system.

Please note that alternative approaches could have been taken in this step, which results in preliminary sizing of the group. Static codes such as FLPIER, or, for example, a simple program known as PIGLET (*45*), could have been employed using an estimated peak dynamic load. However, use of FLPIER(D) in this step is expected to save time in the overall design process.

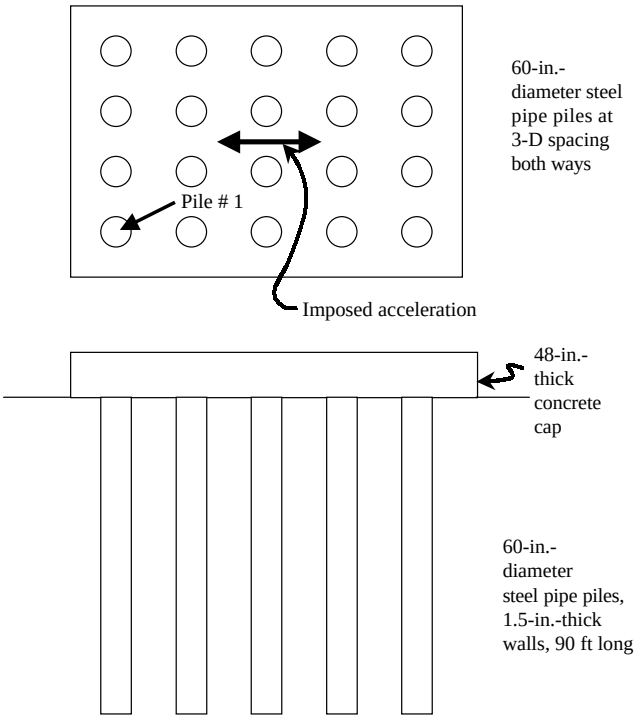

Note: 1 in. = 25.4 mm

Figure 42. Layout of pile group for FLPIER(D) example problem.

Step 4: *Convert the static model to a time-domain dynamic model by adding damping, mass, and an earthquake record.*

The file used for this analysis is included with the example files as part of the FLPier_Dyn install and is named "design_dyn_gap.in." In this phase of the analysis (i.e., the time-domain analysis), damping is handled differently from the way in which it was handled in the previous phase (i.e., the pseudo-dynamic analysis [Step 3]). In the pseudo-dynamic analysis, soil damping was handled in FLPIER(D) by using the approximation developed in Appendix B. In this step, however, hysteretic damping in the soil under lateral loading (with the *p-y* curves) was modeled in FLPIER(D) using the gap model described in Appendix C. There is no hysteretic damping associated with axial loading of the piles as the cap rotates in this example. Radiation damping in this step, for both lateral and axial loading of the piles, was handled in FLPIER(D) by specifying Raleigh damping (*45*). The axial load-movement curves were generated in FLPIER(D) using McVay's (*33*) driven pile model for unit load transfer curves.

In this phase, an earthquake record (i.e., the acceleration time history) was input as a discrete time history at the origin of coordinates (i.e., the middle of the top of the pile cap). The acceleration time history used in this example was the El Centro, California, record of 1940. Any saved

acceleration record can be captured by the user interface for FLPIER(D) and placed in the input file. At present, two records are saved for use by the program: El Centro and Northridge, California.

The results of the field Statnamic tests summarized in Chapter 2 and covered in detail in Appendixes D and E were used to infer input parameters for this phase of the analysis. From the field Statnamic tests, the following parameters appear to work well in the FLPIER(D) model:

- **Damping:** Raleigh damping can be used to replicate radiation damping in the pile group system. Such damping is expressed in FLPIER(D) by ($\alpha \times$ mass of the cap and pile system + $\beta \times$ lateral group stiffness). In the field tests conducted with steel piles, good matching was found with FLPIER(D) using the following, with the exception (for soil) described in the following:

	α	β
Structure (pier)	0.04	0.01
Piles	0.001 (steel)	0.001 (steel)
Soil	0.015	0.015

In the analysis of earthquake motion, additional damping is required that was not found in the Statnamic tests because the Statnamic device applies a short pulse of energy followed by a period of free vibration response. An earthquake acceleration record, however, causes continuous energy input, and the response is more sensitive to damping.

It is estimated that the soil damping is about 10 times that of a steel pile. As a result of Step 3, the damping values shown in the preceding table were used, and the pier and pile group shown in Figure 42 was analyzed.

- **Additional Input Options:** For the dynamic time domain analysis, the following options were specified:
  - **P = 2, 1, 4:** Print displacements for the analysis for Nodes 1 and 4 (i.e., the pile heads). This will create the name.DS1 and name.DS2 files, which contain the six displacements at Nodes 1 and 4, respectively, for each time step. These are text files and are best viewed using a spreadsheet such as Microsoft Excel.
  - **W = 1, 1, 1:** Print the forces for Pile 1, Element 1, and Node 1 (the bottom of the element) for each time step. Only one end of a single element can be printed per run. The forces are saved in the file *name*.DFO.

  All the plots in the list given below were executed using Excel. To read the result files in Excel, do the following:
  1. Start Excel by using the File->Open command;
  2. Change to all files (*.*);
  3. Select the file to read (name.DS1 or name.DFO, etc.); and
  4. On the pop-up dialog, select finish (to read the data).

  All data are now in columns and can be plotted using normal Excel functions.
- **Principal Results from Time-Domain Analysis:** From the dynamic time-domain analysis, plots were made for the pile-head translation in the direction of loading (*X*) and for the induced bending moment in the direction of loading for Pile 1 for the time window of the analysis. These plots are given in Figures 43 and 44, respectively. In both of these figures, time is expressed in seconds.

The maximum displacement in the analysis is a little more than 2 in. (51 mm). Notice that the earthquake response has several significant peaks during the modeled time window of response. Unlike the free vibration response from the Statnamic test, the response does not decay. The moment at the head of Pile 1 is given in Figure 44. Similarly, several peaks occur, and the maximum moment is slightly more than 15,000 in.-K (1695 kN-m),

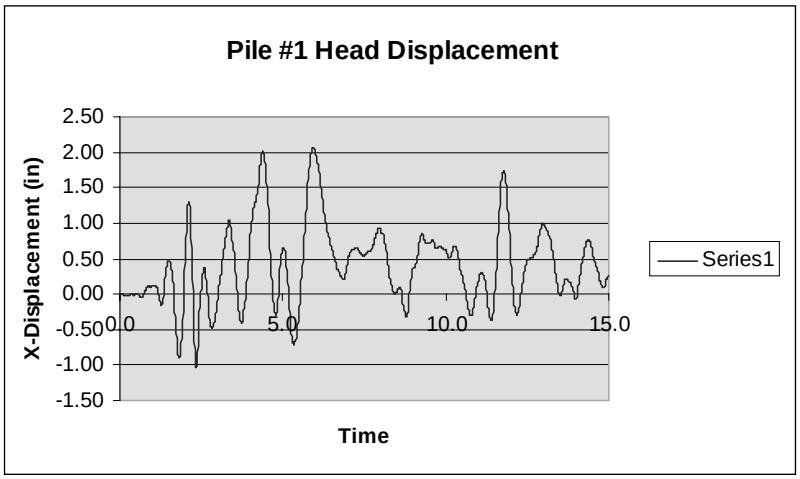

Figure 43. Lateral displacement time history for Pile 1 computed by FLPIER(D).

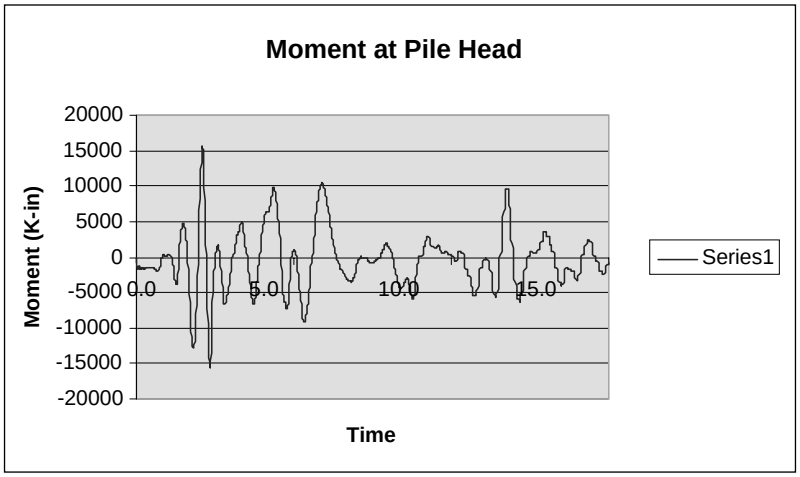

Figure 44. Time history of bending moment computed at the head of Pile 1 by FLPIER(D).

which is less than the moment at which plastic behavior occurs.

Because convergence occurs in FLPIER(D), the piles have sufficient moment capacity. The gap model causes the structure flexibility to increase as time increases because less and less of the soil is in contact with the piles.

- **Completing the Design Process:** This analysis should be conducted *using a range of values* of soil properties that covers the associated uncertainties, including damping and *p*-multipliers. For example, it would be prudent to vary the default *p*-multipliers by about ± 25 percent and to reduce the front-row values to as low as 0.5 for bored piles in cohesionless soil. For critical structures, the design process should include site-specific dynamic pile group loading tests with a large-force exciter to calibrate the program to site conditions.

CHAPTER **4**

CONCLUSIONS AND RECOMMENDATIONS

CONCLUSIONS

The research confirmed the viability of the reusable pile-testing system with the Statnamic activator; however, the original plans for a steel-frame cap proved infeasible for repeated use, and cast-in-place caps are recommended in any future experiments.

From a design perspective, the research demonstrated that laterally loaded pile groups in nonliquefying soil that are exposed to low-frequency (2 to 4 Hz), high-displacement-amplitude (≥ 20 mm) loading, or both, can be simulated using a code such as FLPIER(D), which models the soil with hysteretic, static, *p-y* curves and which uses *p*-multipliers that are derived from static tests (such as the default values in FLPIER or FLPIER[D]). Evidence was presented that the average *p*-multipliers were about 10 percent lower for bored piles in cohesionless soil than the average default values given in FLPIER or FLPIER(D). Inertial effects must be included in the method; however, structural damping has a minor effect on pile group behavior and may be included and omitted, as the designer chooses.

Random variations from the maximum bending moments and shears that were computed for each row of piles by FLPIER(D) were observed in the field experiments. This behavior appeared to derive from random variations in soil stiffness within the group and from other random factors, such as random small batters in the piles. This variability should be accounted for in designing the piles structurally by applying a load factor of approximately 1.2 to the computed maximum moments and shears.

RECOMMENDATIONS FOR FURTHER STUDY

Some modifications to FLPIER—to create the dynamic version FLPIER(D)—are in order:

1. The default parameters in FLPIER(D) tend to overestimate damping, based on comparisons with the impact-type field tests in this study. Adjustments to the unloading branches of *p-y* curves may improve modeling of hysteretic damping for this type of loading. Further studies of the effects of high-amplitude, cyclic dynamic loading should be undertaken to determine whether the FLPIER(D) damping model is suitable for seismic loading without modification.
2. FLPIER(D) gives unexpected results at certain times when the displacement is large and when the piles are prescribed to have partial fixity with the cap. This effect appears to be due to convergence of the mathematical solution and to the sensitivity of the solution to the value of the rotational restraint at the pile head. Corrections have been made in the program to minimize this effect; however, users should proceed with caution when analyzing piles with partial head fixity. This behavior should be investigated further, and the formulations should be corrected, if necessary.
3. FLPIER(D) has not been verified for the case in which loading is generated against the piles from the soil (i.e., kinematic loading with inertial feedback from the superstructure). Further physical data should be collected, perhaps using shaking-table tests or full-scale tests with significant explosive charges, against which to verify FLPIER(D) for this application.
4. An appropriate *p-y* model should be developed to handle liquefying soil.
5. A formal research project should be undertaken to evaluate methods for determining pile-head shear accurately from bending sensors in the piles or by other means and to evaluate the flexural stiffness of pile heads for piles of differing types (e.g., pipe, prestressed concrete, H, circular reinforced concrete) with varied procedures for attaching the piles to the caps. This project, if successful, should make it easier to perform and interpret the results of field tests on laterally loaded pile groups.

With respect to the field testing program, it is noted that the test piles that were instrumented and developed for this study, as well as the Statnamic testing device (which is the property of FHWA) are available for further testing on other sites. The major conclusions of this research, stated above, should be verified by further field tests in other geologic settings (e.g., stiff clay; loose, clean water-bearing sand; loose, dry sand; and soft-over-stiff soil layering). This verification can be accomplished most conveniently in conjunction with highway-construction projects.

The applicability of this research to seismic loading can be enhanced by repeating these experiments, using a large vibra-

tor, to correlate damping inferred from Statnamic tests with damping under continuous loading with nonlinear displacements. Such a vibrator should be designed, constructed, and deployed.

IMPLEMENTATION PLAN

A brief plan for the implementation of this research is as follows:

1. The appropriate federal agency should identify state DOT design projects in which seismic or vessel–ice impact is a major concern in the design of the foundations.
2. Two to four such projects should be selected for research implementation. The selected projects should cover a variety of soil sites (e.g., saturated sand, soft clay, very stiff clay or rock) and more than one type of loading event (e.g., seismic and vessel impact).
3. The custodian of the testing equipment from this project should then be directed to make such equipment available to the state DOTs whose design projects are selected, and those states should conduct full-scale field tests with a Statnamic device, as was employed in this project, or with a very large vibrator.
4. The state DOTs or their consultants should, in parallel with the field tests, perform mathematical modeling of the test pile group using either FLPIER(D) or other suitable software, taking advantage initially of the recommendations developed in this report and modifying the input parameters as necessary to affect acceptable matches with the observations. The same software should then be used to design the pile foundations for the subject structure.
5. During this process, the responsible federal agency should compile the results of the field tests and of the designers' interpretations for input parameters (i.e., damping values, *p*-multipliers, etc.) and should make the information available to the national community of DOT structural and geotechnical engineers through a sponsored conference or short course.
6. The use of the field testing system developed for the current project and the software that is used in the above process should then be evaluated by a select panel of experts, and a decision should be made by the responsible federal agency, with the advice of the panel of experts, whether to continue with further field experiments, to standardize the input parameters (so as to use them without field testing), or take some other approach to the design of laterally loaded pile groups.

REFERENCES

1. Earthquake Engineering Research Institute. "Loma Prieta Earthquake Reconnaissance Report," Chapter 6: Bridge Structures in *Earthquake Spectra, Supplement to Volume 6* (1990); pp. 151–187.
2. Buckle, I. G. *The Northridge, California, Earthquake of January 17, 1994: Performance of Highway Bridges.* Technical Report NCEER-94-0008, National Center for Earthquake Engineering Research (1994).
3. Earthquake Engineering Research Institute. "Northridge Earthquake of January 17, 1994, Reconnaissance Report," Chapter 6: Highway Bridges and Traffic Management in *Earthquake Spectra, Supplement to Volume 11* (1995); pp. 287–372.
4. Kiremidjian, A. A., and N. Basoz. "Evaluation of Bridge Damage Data from Recent Earthquakes," *NCEER Bulletin*, National Center for Earthquake Engineering Research, Vol.11, No. 2 (1997); pp. 1–7.
5. Buckle, I. G. "Report from the Hanshin-Awaji Earthquake: Overview of Performance of Highway Bridges," *NCEER Bulletin*, National Center for Earthquake Engineering Research, Vol. 9, No. 2 (1995); pp. 1–6.
6. Costantino, C. "Report from the Hanshin-Awaji Earthquake: Overview of Geotechnical Observations," *NCEER Bulletin*, National Center for Earthquake Engineering Research, Vol. 9, No. 2 (1995); pp. 7–10.
7. Ishihara, K. "Geotechnical Aspects of the 1995 Kobe Earthquake," *Proceedings, XIV International Conference on Soil Mechanics and Foundation Engineering*, Vol. 4, Hamburg; Balkema (1997); pp. 2047–2073.
8. Matsui, T., M. Kitazawa, A. Nanjo, and F. Yasuda. "Investigation of Damaged Foundations in the Great Hanshin Earthquake Disaster," *Seismic Behavior of Ground and Geotechnical Structures*, P. S. Sêco e Pinto (ed.); Balkema (1997); pp. 235–242.
9. Lin, M.-L. *Geotechnical Hazard Caused by Chi-Chi Earthquake*. Department of Civil Engineering, National Taiwan University (2000).
10. *Chi-Chi Earthquake Database Analysis and Management System (CEDAMS)*. Taiwan's National Center for Research and Earthquake Engineering, Taipei (2000).
11. Chang, K.-C., D.-W. Chang, M.-H. Tsai, and Y-C. Sung. "Seismic Performance of Highway Bridges," *Earthquake Engineering and Engineering Seismology*, Vol. 2, No. 1 (2000); pp. 55–77.
12. Bardet, J. P., N. Adachi, I. M. Idriss, M. Hamada, T. O'Rourke, and K. Ishihara. Chapter 7: Performance of Pile Foundations in *Proceedings, North America–Japan Workshop on the Geotechnical Aspects of the Kobe, Loma Prieta, and Northridge Earthquakes*. National Science Foundation, Air Force Office of Scientific Research, Japanese Geotechnical Society (1997).
13. O'Neill, M. W., D. A. Brown, D. G. Anderson, H. El Naggar, F. Townsend, and M. C. McVay. "Static and Dynamic Lateral Loading of Pile Groups," Interim Report for NCHRP Project 24-9. National Cooperative Highway Research Program, Transportation Research Board (1997).
14. Budek, A. M., M. J. N. Priestley, and G. Benzoni. "The Inelastic Seismic Response of Bridge Drilled-Shaft RC Pile/Columns," *Journal of Structural Engineering*, ASCE, Vol. 126, No. 4 (2000); pp. 510–517.
15. Davisson, M. T. "Lateral Load Capacity of Piles," *Highway Research Record 333*, Highway Research Board, National Research Council (1970); pp. 104–112.
16. *Foundations and Earth Structures—Design Manual 7.2*. NAVFAC DM-7.2. Department of the Navy, Naval Facilities Engineering Command (1982).
17. *Canadian Foundation Engineering Manual* (2nd Edition). Canadian Geotechnical Society, Bitech Publishers Ltd. (1985).
18. *AASHTO Bridge Design Specifications*. American Association of State Highway and Transportation Officials (1996).
19. *Design of Pile Foundations—Technical Engineering and Design Guides No. 1*. ASCE, adapted from the U.S. Army Corps of Engineers (1993).
20. Poulos, H. G., and E. H. Davis. *Pile Foundations Analysis and Design*. Wiley (1980).
21. PoLam, I., and G. R. Martin. *Seismic Design of Highway Bridge Foundations, Volume II: Design Procedures and Guidelines*, Report No. FHWA/RD-86/102. U.S.DOT, FHWA (1986).
22. *Improved Seismic Design Criteria for California Bridges* (ATC-32), Contract 59N203. Applied Technology Council (1996).
23. Williams, M. E., C. Fernandes Jr., and M. I. Hoit. "Comparison of Dynamic Analysis Methods for Bridge Piers," *Journal of Bridge Engineering*, ASCE, in review (2001).
24. PoLam, I., M. Kapuskar, and D. Chaudhuri. *Modeling of Pile Footings and Drilled Shafts for Seismic Design*, Technical Report MCEER-98-0018. Multidisciplinary Center for Earthquake Engineering Research, State University of New York at Buffalo (1998).
25. Reese, L. C., and S. T. Wang. *Computer Program LPILE Plus*, Version 3.0, Technical Manual. Ensoft, Inc. (1997).
26. *PAR: Pile Analysis Routines: Theoretical and User's Manuals*. PMB Engineering, Inc. (1988).
27. *Design Manual for Foundation Stiffnesses Under Seismic Loading*. Prepared for Washington State DOT by Geospectra (1997).
28. Schnabel, P. B., J. Lysmer, and H. B. Seed. *SHAKE: A Computer Program for Earthquake Response Analysis of Horizontally Layered Sites*, Report EERC 72-12. University of California Earthquake Engineering Research Center (1972).
29. Norris, G. M. "Seismic Bridge Pile Foundation Behavior," in *Proceedings, International Conference on Design and Construction of Bridge Foundations*, FHWA, Vol. 1 (1994); pp. 27–136.
30. Ashour, M. A., G. Norris, and P. Pilling. "Lateral Loading of a Pile in Layered Soil Using the Strain Wedge Model," *Journal of Geotechnical and Geoenvironmental Engineering*, ASCE, Vol. 124, No. 4 (1998); pp. 303–315.
31. Ashour, M. A., and G. Norris. "Modeling Lateral Soil-Pile Response Based on Soil-Pile Interaction," *Journal of Geotechnical and Geoenvironmental Engineering*, ASCE, Vol. 126, No. 5 (2000); pp. 420−428.
32. Peterson, K., and K. M. Rollins. *Static and Dynamic Lateral Load Testing of a Full-Scale Pile Group in Clay*, Research

Report CEG.96-02. Department of Civil Engineering, Brigham Young University (1996).
33. McVay, M., C. Hays, and M. Hoit. *User's Manual for Florida Pier*, Version 5.1. Department of Civil Engineering, University of Florida (1996).
34. Dobry, R., A. Abdoun, and T. D. O'Rourke. "Evaluation of Pile Response Due to Liquefaction Induced Lateral Spreading of the Ground," in *Proceedings, 4th Caltrans Seismic Design Workshop*, Sacramento (1996).
35. Wilson, D. W., R. W. Boulanger, B. L. Kutter, and A. Abghari. "Soil-Pile Superstructure Interaction Experiments with Liquefiable Sand in the Centrifuge," in *Proceedings, 4th Caltrans Seismic Design Workshop*, Sacramento (1996).
36. Ashford, S. A., and K. Rollins. "Full-Scale Behavior of Laterally Loaded Deep Foundations in Liquefied Sand: Preliminary Test Results," Preliminary Report. Department of Structural Engineering, University of California, San Diego (1999).
37. Randolph, M. F., and H. G. Poulos. "Estimating the Flexibility of Offshore Pile Groups," in *Proceedings, 2nd International Conference on Numerical Methods in Offshore Piling*, Austin (1982); pp. 313–328.
38. Bathe, K. J. *ADINA User's Manual*, ADINA R and D, Inc. (1998).
39. *General Finite Element Analysis Program*, Version 5.4. ANSYS, Inc. (1996).
40. El Naggar, M. H., and M. Novak. "Nonlinear Analysis for Dynamic Lateral Pile Response," *Journal of Soil Dynamics and Earthquake Engineering*, Vol. 15, No. 4 (1996); pp. 233–244.
41. "Recommended Practice for Planning, Designing and Constructing Fixed Offshore Platforms," *API Recommended Practice 2A* (19th edition). American Petroleum Institute (1991); pp. 47–55.
42. Matlock, H. "Correlations for Design of Laterally Loaded Piles in Soft Clays," *Proceedings, Second Annual Offshore Technology Conference*, Houston (1970); pp. 578–588.
43. Reese, L. C., W. R. Cox, and F. C. Koop. "Analysis of Laterally Loaded Piles in Sand," *Proceeding, Offshore Technology Conference*, Houston (1974); pp. 473–484.
44. Sowers, G. F., and T. L. Richardson. "Residual Soils of the Piedmont and Blue Ridge." *Transportation Research Record No. 919.* Transportation Research Board, National Research Council (1983); pp. 10–16.
45. Randolph, M. F. *PIGLET: A Computer Program for the Analysis and Design of Pile Groups Under General Loading Conditions*, Soil Report TR91 CUED/D. Cambridge University (1980); (currently available from the Department of Civil Engineering, University of Western Australia).

APPENDIX A

COMPARATIVE BEHAVIOR OF LATERALLY LOADED GROUPS OF BORED AND DRIVEN PILES

INTRODUCTION

The soil modeling approach that has been adopted in this research is to simulate lateral group behavior by (1) using *p-y* curves for statically loaded single piles from well-known criteria (e.g., *1, 2*)—these criteria are resident in many design-level computer codes and are easy for the designer to implement (e.g., *3–5*); (2) converting the static *p-y* curves into dynamic *p-y* curves if seismic or impact loading is being modeled (see Appendix B); and (3) modifying single-pile curves for lateral group action by using a *p*-multiplier, which may be either a static factor (as discussed in this appendix) or a dynamic factor (as discussed in Appendix B). The *p*-multiplier approach is used in the Florida Pier Program (FLPIER) (*4, 5*), modified for dynamic loading as described in Appendix C.

Values for *p*-multipliers have been evaluated through detailed numerical or analytical modeling or by performing load tests on pile groups, or by a combination of both numerical or analytical modeling and field or centrifuge tests (*6–10*). However, none of these studies has been specific to the construction method that is used to install the piles. The contribution of this appendix is to describe a major field load test program in which the effect of the piling construction method on *p*-multipliers was evaluated.

TEST SITE AND TEST ARRANGEMENT

Site Conditions

In planning for the construction of foundations for numerous viaducts to support rail traffic through the west central coastal plain of Taiwan, the High Speed Rail Authority of Taiwan contracted with several universities, consulting firms, and contractors to construct and load test two large, full-scale pile groups. The west central coastal plain of Taiwan is in a geographical area that is prone to large seismic events, and it was considered necessary to design the viaducts to resist large horizontal loads.

The objective of the test program was to measure the capacity and stiffness of groups of vertical piles of different designs that were loaded laterally with a quasi-static ground-line shear. Two test groups were selected for construction and testing. The cost of construction for each group was estimated to be approximately equal. These groups were constructed and loaded to the capacity of the loading system, 1000 metric tons ("T") (9.8 MN). One pile group consisted of bored piles (drilled shafts), and one consisted of round, displacement-type prestressed concrete piles, which were driven into position.

The test site was located about 5 km west of the town of Chaiyi, Taiwan, on a flat coastal plain. Soil conditions at the test site are summarized in Figure A-1. The ground surface shown in that figure is the elevation of the ground surface at the base of the pile caps of the tested groups after minor excavation. Detailed soil data are available in Reference 11. Made on the test site, within 5 m of each test group, were numerous geophysical tests; soil borings; and cone penetration test (CPT), standard penetration test (SPT), and dilatometer test (DMT) soundings. The Unified classifications of the soil layers and the various parameters listed in the "Properties" column of Figure A-1 were deduced from the borings and soundings (*11*). The piezometric surface was located at 3 m below the ground surface. The soils in the top 8 m of the profile are considered to be "sands" with a relative density of 50 to 60 percent in the following analysis.

Testing Arrangement

The layouts of the test groups are shown in Figures A-2 and A-3. All piles were plumb to the tolerances permitted by the High Speed Rail Authority (i.e., 2 percent). The lateral load tests were conducted essentially by jacking the two test groups apart. That is, the test groups served as mutual reactions for each other.

Bored Pile Group

The bored pile group (see Figure A-2) consisted of six 1.5-m-diameter piles installed to a depth of 33 to 34 m below the ground surface. All six of the group piles were constructed using the slurry displacement method of construction, in which a bentonite slurry was used to maintain borehole stability. Several other bored piles were constructed, as shown in Figure A-2. Piles B1 and B2 served as reference piles for lateral loading (tested as single, isolated piles). They were tested individually with free heads. Pile B10 served as a reference pile for axial loading. (Piles B9 and B11 served as anchor piles for the axial loading test on Pile B10. The group cap served as the reaction for the lateral load tests on Piles B1 and B2.) Only Pile B1 was constructed by the slurry displacement method, as per the group piles. Piles B2 and B10 (which are highlighted in Figure A-2 with boldface) were constructed using the oscillated casing method, in which casing is oscillated into the soil continuously for the full depth of the borehole, and the soil within the casing is excavated while maintaining a balance on the water head at the base of the casing

Depth m	Boring Log	Description	SPT N averaged	Properties
0	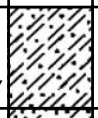	Fine sandy silt; yellowish brown loose with some clayey silts (SM)	5	$k = 27.14$ MN/m^3 $\phi = 35°$ $\gamma = 19$ kN/m^3
3 ▽		Silty fine sand; grey; medium dense; occasionally with sandy silt layers. (SM)	6	$k = 18.86$ MN/m^3 $\phi = 35°$ $\gamma' = 9.2$ kN/m^3
8		Silty clay; greyish brown; medium stiff, occasionally with coarse sand seams (2–3 mm) (CL)	10	$S_u = 60$ kN/m^2 $\varepsilon_{50} = 0.007$ $\gamma' = 9.2$ kN/m^3
12		Silty fine sand; grey; loose with fine sandy silt layer (SM)	10	$k = 18.32$ MN/m^3 $\phi = 34°$ $\gamma' = 9.4$ kN/m^3
17		Clayey silts; grey; medium dense with little sandy silts (ML/CL) Silty clay; grey; medium dense with silty fine sand layer	17	$k = 20.36$ MN/m^3 $\phi = 34°$ $\gamma' = 9.2$ kN/m^3
25		Silty clay; grey; very stiff with little fine sand (CL)	18	$S_u = 115$ kN/m^2 $\varepsilon_{50} = 0.005$ $\gamma' = 9.2$ kN/m^3
32		Silty clay; grey; very stiff with silty fine sand layer (SM/CL)	19	$S_u = 121.3$ kN/m^2 $\varepsilon_{50} = 0.005$ $\gamma' = 9.2$ kN/m^3
43			45	

Figure A-1. Subsurface profile at Chaiyi, Taiwan, test site.

throughout the process. The reinforcing steel is then set, and the borehole is concreted using temie techniques as the casing is withdrawn, similar to the way in which a borehole is concreted during the construction of bored piles by the slurry displacement method. Because Pile B2 was constructed in a manner different from the group piles, results from the test on Pile B1 were used exclusively in the analysis that is described in this appendix. The axial load test results on Pile B10 were used only in a general way to confirm the approximate correctness of the axial load model that is needed for the analysis of laterally loaded pile groups with nonpinned heads.

A potentially important detail is the order in which the piles were installed. In very general terms, the bored piles in the group were installed from the front, or leading, row (i.e., first) to the back, or trailing, row (i.e., last). It is speculated that this installation order might have resulted in reduced effective stresses in the coarse-grained soil surrounding the piles that were installed first—those in the leading row—by the later installation of piles behind the leading row. Reduced effective

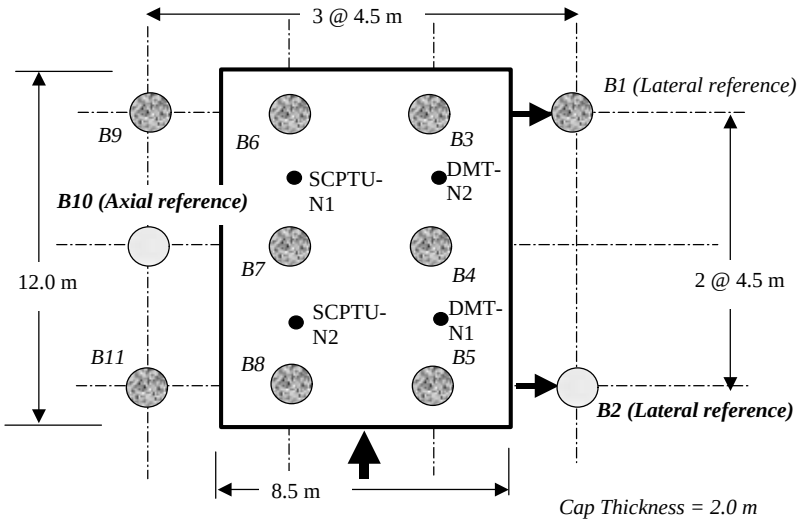

(a) Bored pile group layout.

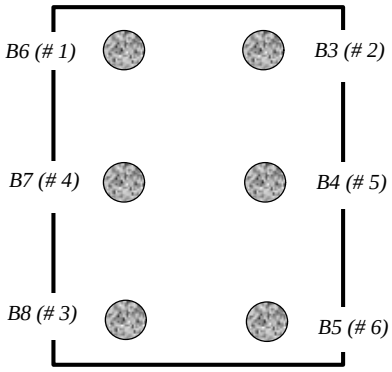

(b) Order of installation for bored piles in test group.

Figure A-2. Plan view of test group for bored piles and reference piles (not to scale).

stresses in the soil mass around the front-row piles should have produced softer soil response behavior of the leading-row piles compared with the behavior that might have occurred if the leading row of piles had been installed last.

Driven Pile Group

The driven pile group consisted of 12 0.80-m-diameter, closed-toe, hollow, circular prestressed concrete piles. They were also driven to a penetration of 33 to 34 m. These piles can be considered to be "displacement piles." The hollow core of each pile was filled with an instrument package and concrete after all of the piles were installed. A single, isolated pile, denoted P13 in Figure A-3, was tested laterally in a free-headed state by reacting off the group pile cap. Before the cap was constructed, Piles P6 and P7 were subjected to axial load tests. Because of the assumptions concerning head fixity in the driven pile group, which is discussed later, it was not necessary to model the axial load behavior of the group piles with close accuracy.

The installation order of the driven piles is also shown in Figure A-3. The order of installation was more random than that of the bored pile group; however, in general, the piles on the leading row were installed prior to the piles on the second (i.e., first trailing) row, which were in turn installed prior to the piles in the third (i.e., second trailing) row. The piles on the fourth (i.e., third trailing) row were installed last. With displacement-type piles in coarse-grained soil, it can be speculated that the effect of installing the leading row first was opposite to the effect of installing the leading row first in the bored pile group. That is, installing displacement piles in a row behind a row of piles already installed would increase effective stresses around the piles already installed and would

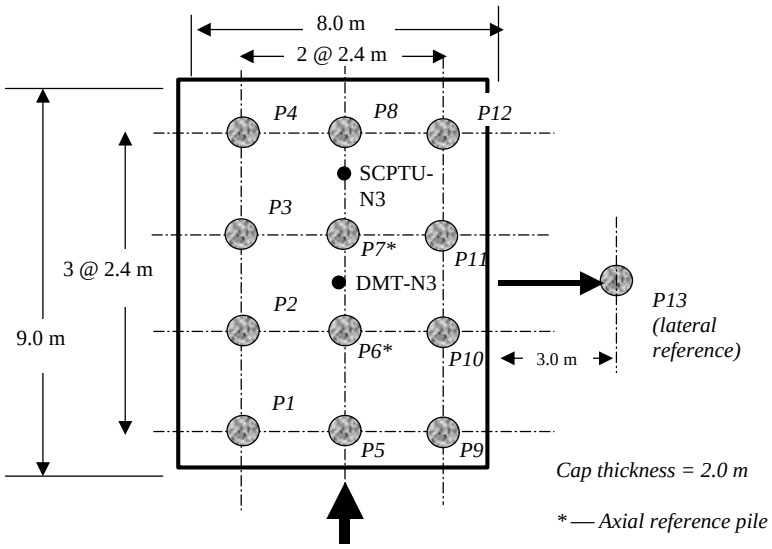

(a) Driven pile group layout.

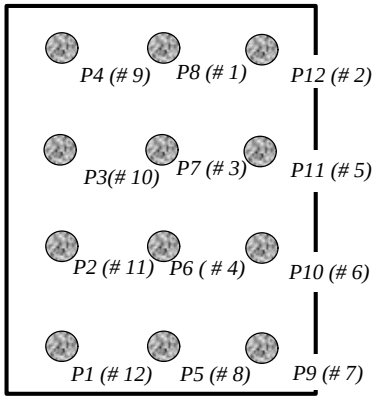

(b) Order of installation for driven piles in test group.

Figure A-3. Plan view of test group for driven piles and reference piles (not to scale).

result in stiffer soil response in those piles than in the piles installed later.

Instrumentation

Both the bored and driven piles were instrumented thoroughly. The piles that were subjected to individual pile axial load tests were instrumented with a toe load cell, a family of telltales and rebar stress meters (referred to in the United States as "sister bars"). The piles that were subjected to lateral load tests, including all of the group piles and the lateral reference piles, were instrumented with inclinometer tubing on approximately the neutral axis of the pile. Deviations in lateral deflection from the pile toes (which are considered to be stationary) were measured with precision inclinometers during the load tests. Some of the piles that were loaded laterally also contained sister bars. The translations and rotations of the group caps were measured by using linear variable differential transformers suspended from reference frames supported in the soil as far from the test groups as possible. The load was applied to the group by multiple hydraulic jacks whose loads were controlled in order to "steer" the group on an approximately straight path. Each jack was equipped with a calibrated electronic load cell.

The instruments for the bored piles were affixed to the reinforcing steel cages prior to inserting the cages into the boreholes and concreting the piles. The instruments for the driven piles were installed in the hollow core of each pile by attaching the instruments to a carrier and lowering the carrier into the core after the piles were driven. The operation was completed by concreting the instruments into the core.

The interpretations given here are based on the jack load cell, cap-deflection, and inclinometer readings. Sister-bar readings, although available, were not used because not all piles had sister bars and because initial review of the readings revealed some inconsistencies that could not be explained by the individuals reviewing the data.

More information on the instrumentation and pile-group arrangements can be found in Reference 12 (*12*).

Single-Pile Tests

General Description

The single-reference piles (i.e., B1, B2, and P13) were all tested statically, free-headed, by applying a horizontal load approximately 0.5 m above the ground surface. The geomaterials from that level to the ground surface were removed in the analyses that follow. The individual test piles were all subjected to forced vibration tests to load amplitudes as high as 44.5 kN (5 tons) prior to the static load tests. Because these loads were comparatively small, it has been assumed that they had minimal effect on the load-movement behavior that was measured in the static tests. The loads were applied to the single piles by reacting off the respective group pile caps, prior to loading the pile groups, in a direction perpendicular to the direction of group loading. Again, it was assumed that the loading of the single piles in this manner had no effect on the measured response of the pile groups.

The single pile load tests were performed from May 29 through 31, 1997, approximately 5 months after the piles were installed. Loads were applied semi-monotonically. That is, loads were applied in increments until the load reached approximately one-seventh of the expected capacity, at which time the load was removed. The process was repeated for loads equal to about two-sevenths of the expected capacity, three-sevenths of the expected capacity, and so forth, until the final capacity was reached. Readings that were made near the peak loads on each cycle are reported in this appendix as it was assumed that the lateral pile response at such loads was not significantly influenced by cycling at lower load amplitudes.

The load deformation depth relations that were measured for Piles B1 (i.e., the reference for the bored pile group test) and P13 (i.e., the reference for the driven pile group test) are shown in Figures A-4 and A-5, respectively. In these figures, the symbol "T" represents metric tons (or tonnes) rather than U.S. tons, where 1 T = 9.8 kN. As stated previously, Pile B2 was not used as a reference because it was installed using the oscillated casing procedure rather than using the slurry displacement procedure, which was used for all of the group piles. As would be expected, the bored pile, B1, carried considerably more load at a given head deflection than did the driven pile, P13, because of B1's much larger moment of inertia. For the same reason, significant lateral pile movement occurred to a greater depth in the reference bored pile (about 7 m) than in the reference driven pile (about 5 m).

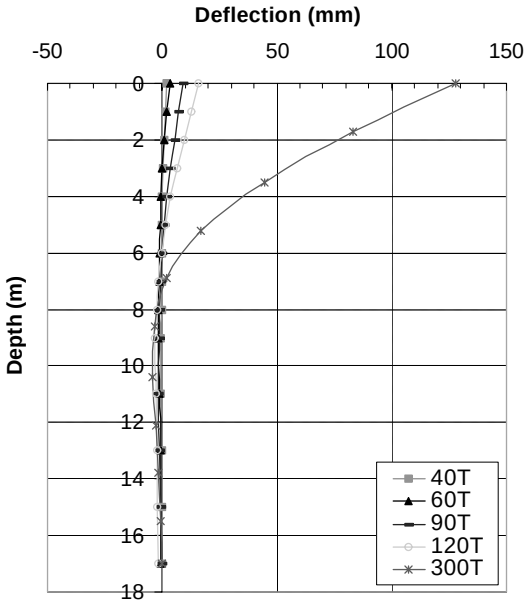

Figure A-4. Measured load deflection depth relations for Pile B1.

Analysis of Single Pile–Test Results

From the perspective of this appendix's objective, the main purpose of the single-pile tests was to establish site-specific, pile geometry–specific, and construction method–specific *p-y* curves for the reference piles. The pile-and-soil profile that was assumed for the analysis of the single pile–load tests is shown in Figure A-6. The soil was modeled initially by using standard *p-y* curve formulations—that of Reese et al. (*1*) for

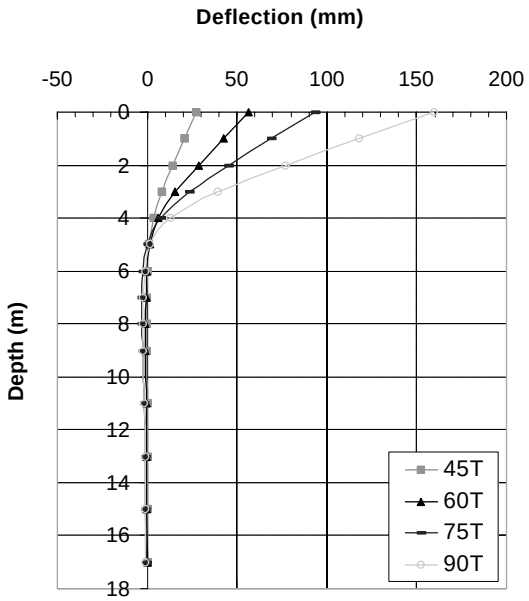

Figure A-5. Measured load deflection depth relations for Pile P13.

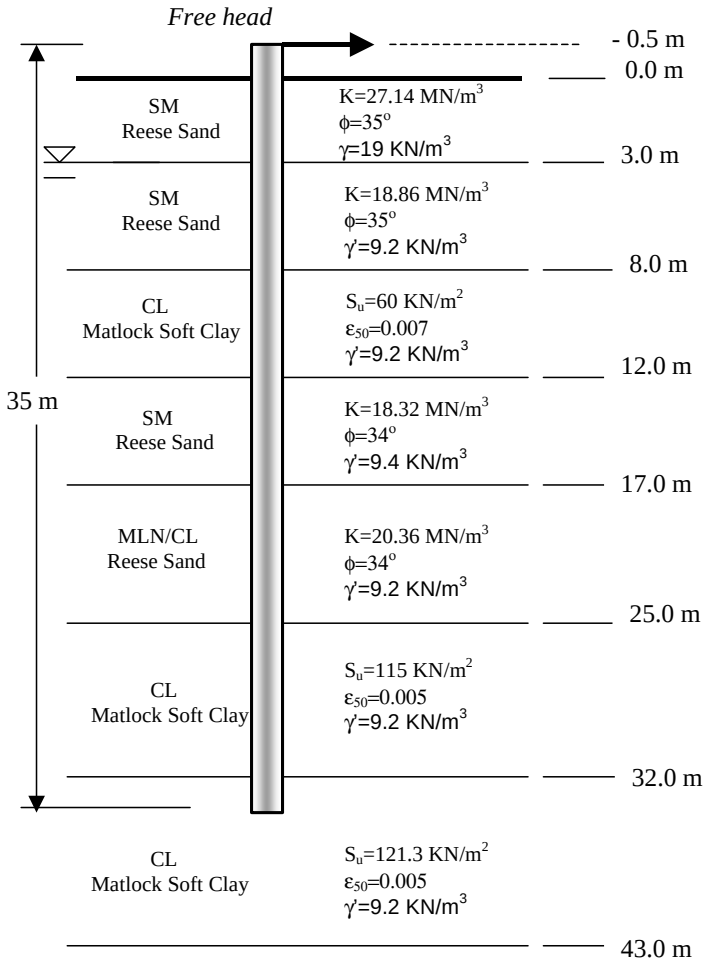

Figure A-6. Soil properties used in developing initial p-y *curves.*

coarse-grained soil layers (i.e., sand) and that of Matlock (*13*) for fine-grained (i.e., clay) soil layers. In preliminary analyses, the Murchison and O'Neill (*2*) *p-y* criterion was also used for the sand layers, in place of the Reese et al. criterion; however, the predictions of deformed pile shape was better with the Reese et al. criterion, so the Reese et al. criterion was used as the starting point for the analysis.

Modeling of the structural properties of the piles is at least as important as modeling the resistance-deformation behavior of the soil (i.e., through *p-y* curves). Simplified design drawings for a typical bored pile and a typical driven (prestressed concrete) pile are shown in Figures A-7 and A-8, respectively. Material properties of the concrete and steel are given in Table A-1. (These were the target properties that were verified from concrete cylinder tests for cast-in-place concrete and steel coupon tests on reinforcing steel. No verification was available for the properties of the concrete in the prestressed outer shell of the driven piles or for the prestressing steel.) The concrete–steel model was the model proposed by Andrade (*14*) and implemented in the version of FLPIER used in this study (*15*). This model computes bending stiffness along the pile by first computing strains across the cross section of a bending element (representing the pile) and assigns corresponding stresses based on uniaxial stress-strain curves for concrete and steel in compression and tension. The gapping-unloading-reloading (hysteretic) structural model described in Appendix C was not resident in the version of FLPIER used in these analyses (i.e., Version 5.1); however, because of the procedure by which the tests were conducted, the gapping-unloading-reloading phenomenon should have had little effect on the pile deflections at the loads at which the tests, both single-pile and group, were analyzed (at or near the peak load in a cycle).

When the tests were first analyzed with FLPIER using the Reese et al. (*1*) and Matlock (*13*) *p-y* criteria for the soil and the Andrade (*14*) structural model for the piles, relatively poor comparisons with the measurements were achieved. Modifications to the *p-y* criteria in the upper 12.0 m of the soil profile were then made in order to improve the match in measured versus computed displaced configuration at several selected loads; that is, site-specific *p-y* curves were determined. The diameters of all bored piles (including the group piles discussed later) were increased in FLPIER from 1.5 to 1.60 m

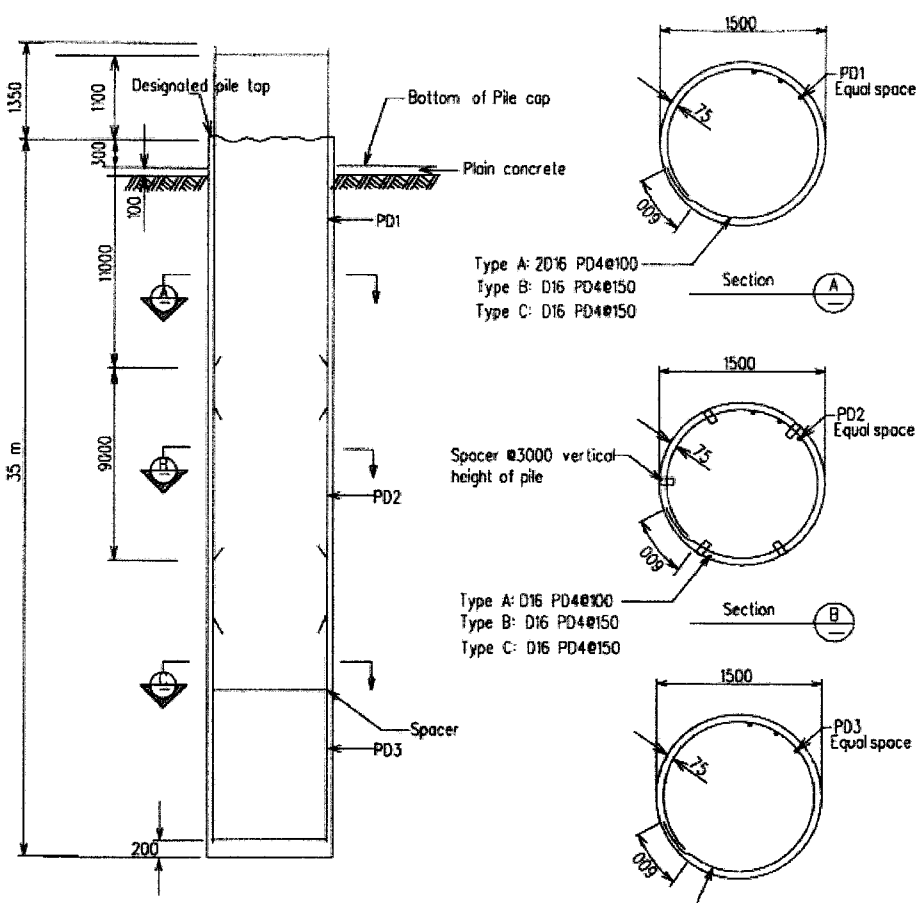

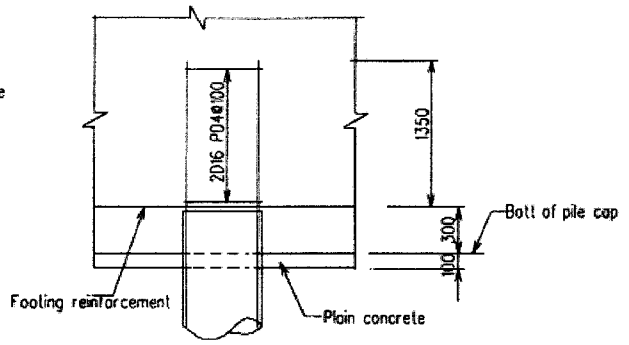

Pile&Pile Cap Connection Detail

Table of Reinforcement A,B,C

NO.	Nominal Diameter	Reinforcement Type	Remark
PD1	D32	———	Type A: 26x3 B: 34 C: 26
PD2	D32	———	Type A: 26x2 B: 34 C: 26
PD3	D32	———	Type A: 26 B: 17 C: 13
PD4	D16	○	

Notes

1 unit: mm except those denoted

2 f_c of concrete=27500 kN/m² ; f_y of steel =411600 kN/m²

3 The reinforcement of bored piles B3-B8 & 12,13 is type A;
B1,2,9&11 is type B; B10 is type C

4 L: the length of bored piles were described inconsistentiy in the series of reports of this project, in this analysis, they are assumed to be 35 m for the single bored pile and 1.5 m shorter for the group piles according to the graphs in the data report.

5 E_c =2x10⁸ kN/m² ; E_s =2.5x10⁷ kN/m²

Figure A-7. Structural details for bored piles.

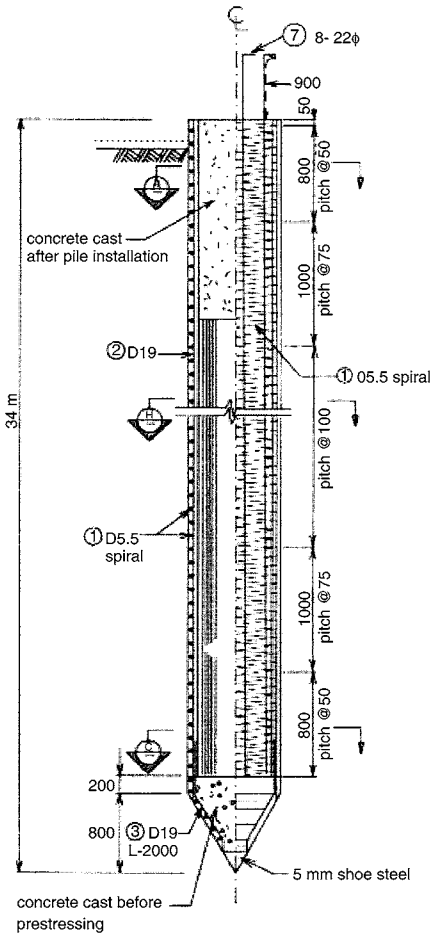

Prestressed Pile Details

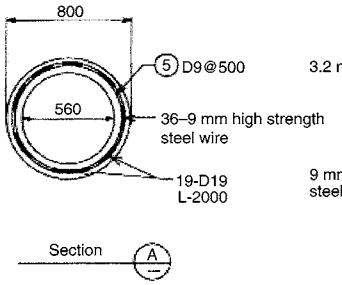

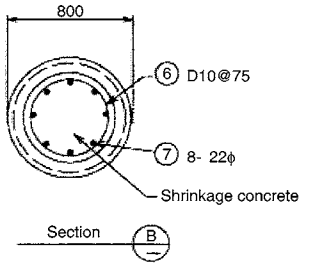

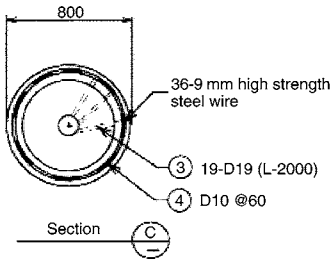

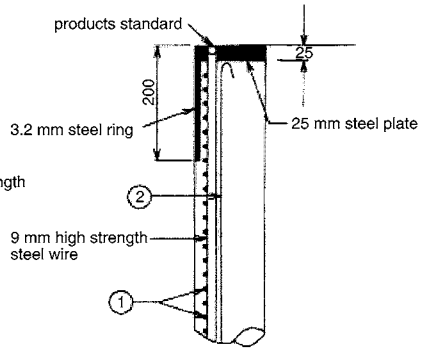

Pile Top Detail

Table of Reinforcement

NO.	Nominal Diameter	Reinforcement Type	Remark
①	D5.5		
②	D19		19
③	D19		19
④	D10		@60
⑤	D9		@500
⑥	D10		@75
⑦	D22		8

Notes

1 PC piles of this project are pretensioned spun concrete piles

2 Ib of concrete: outer material 800 kg/cm^2 (78400 kN/m^2)
core material 210 kg/cm^2 (20580 kN/m^2)

3 Tension strength of 9 mm steel wire area f_w = 14500 kg/cm^2 (1421000 kN/m^2)
f_g = 12500 kg/cm^2 (1225000 kN/m^2)

4 Effective stress transferred to concrete = 80 kg/cm^2 (7840 kN/m^2)

5 L = 34m

6 Es = 2 x 10^3 kN/m^2; Ec = 3.35 x 10^7 kN/m^2

Figure A-8. Structural details for driven (prestressed concrete) piles.

TABLE A-1 Concrete and steel properties for Chaiyi load tests

Property	Bored Piles and Cap	Prestressed Concrete Piles
f'_c (concrete)	27.5 MN/m^2	78.4 MN/m^2 (shell) 20.59 MN/m^2 (core)
E_c (concrete)	2.5 X 10^4 MN/m^2	3.35 X 10^4 MN/m^2 (shell) No data for core (2.0 X 10^4 MN/m^2 used)
f_y (steel)	411.6 MN/m^2	1421 MN/m^2 (cable)
E_s (steel)	199.8 GN/m^2	199.8 GN/m^2

to account for the oversizing of the borehole that commonly occurs when excavating a bored pile in coarse-grained soil under a drilling slurry. The *p-y* curves derived from the original published criteria are compared with the modified *p-y* criteria that were necessary to provide acceptable matches with the measured data in Figures A-9, A-10, and A-11 for Piles B1, B2, and P13, respectively.

One modification to the *p-y* curves was to prescribe a non-zero resistance at the soil surface. This modification is contrary to the Reese et al. sand criterion, which provides for zero soil resistance at the surface. It is not clear what physical phenomenon this change reflected. The surface soil (see Figure A-1) was described as a "sandy silt with some clayey silts," even though it classified as an SM (i.e., silty sand) according to the Unified classification system. It is possible that the need to give the soil surface resistance could reflect a cohesion component to shear strength of the soils not reflected by the Reese et al. sand criteria. A more likely condition, however, was that the bored piles were greater than 1.6 m in diameter at the surface because of the effects of auger drilling and that the need to give the soil non-zero surface resistance actually simulated increased bending stiffness in a pile with a "mushroom" top. The salutary effect of using a non-zero surface resistance *p-y* curve, as shown at the soil surface in Figures A-9 through A-11, versus using null *p-y* curves at the surface, is demonstrated in Figure A-12.

The original and modified *p-y* curves necessary to model Pile B2 (see Figure A-10) were included, even though the data

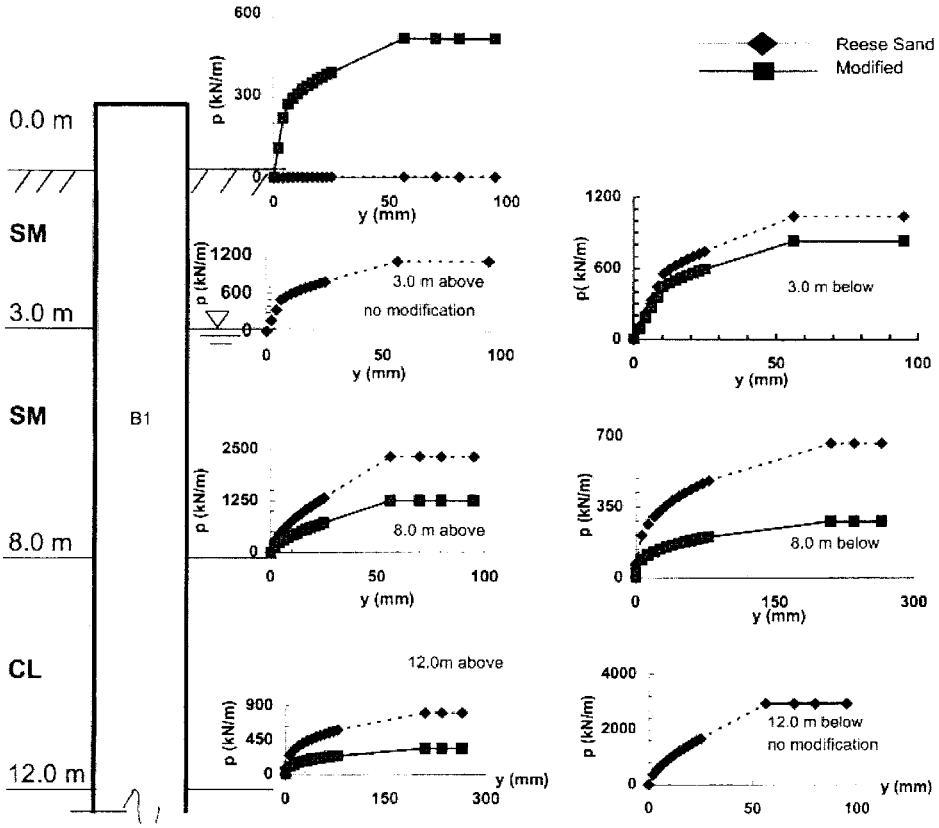

Figure A-9. Original and modified p-y *curves for Bored Pile B-1 (slurry drilled).*

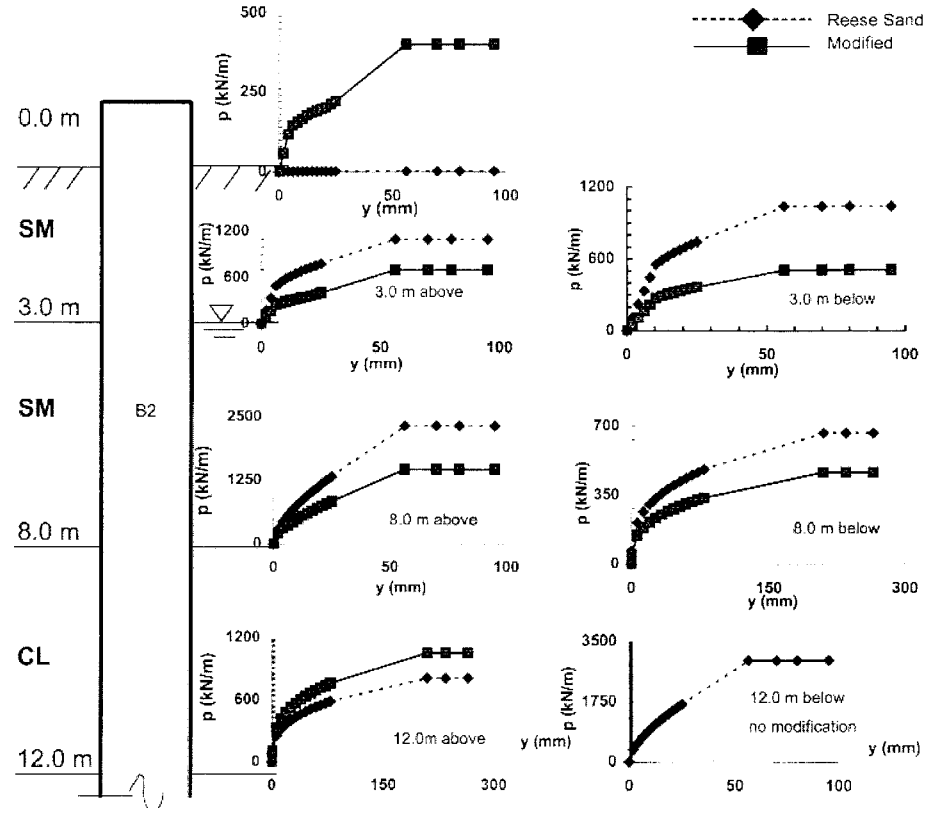

Figure A-10. Original and modified p-y *curves for Bored Pile B2 (full-depth casing).*

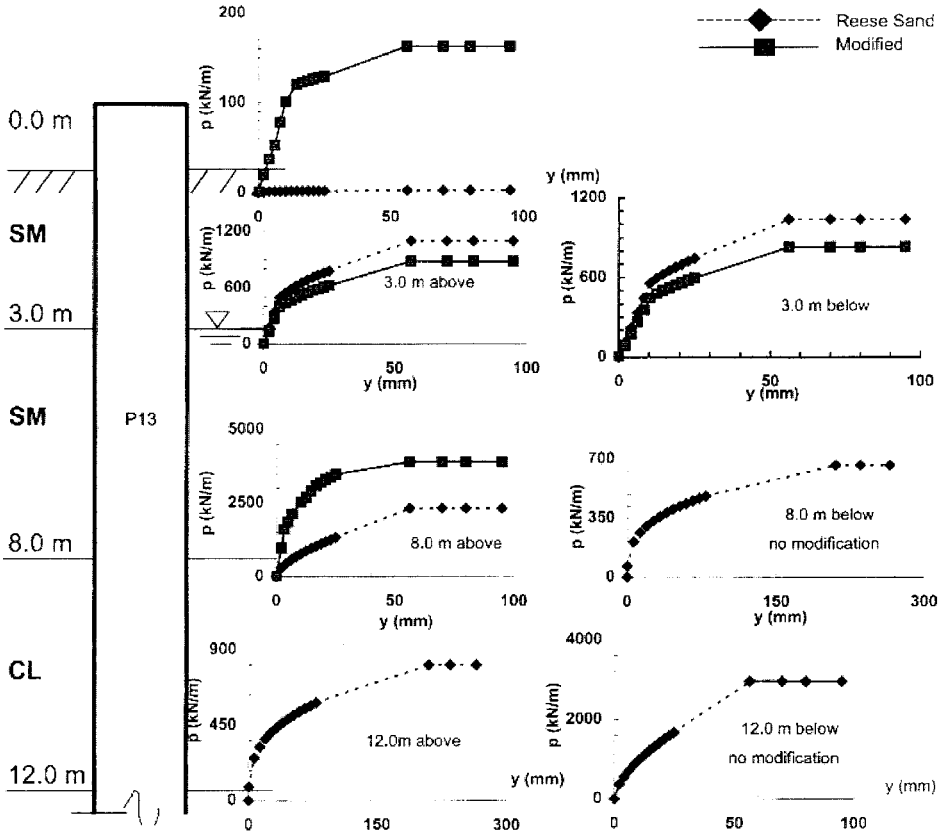

Figure A-11. Original and modified p-y *curves for Driven Pile P13 (prestressed concrete).*

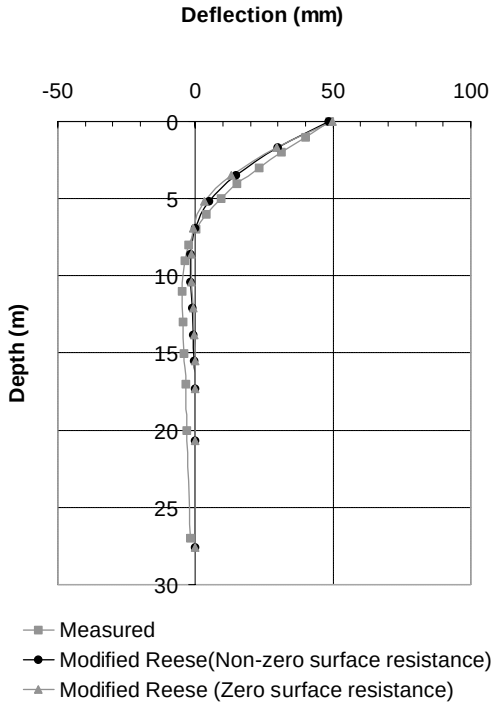

Figure A-12. Effect of p-y *formulation on deflected shape of Bored Pile B1—load = 200 T (1.96 MN).*

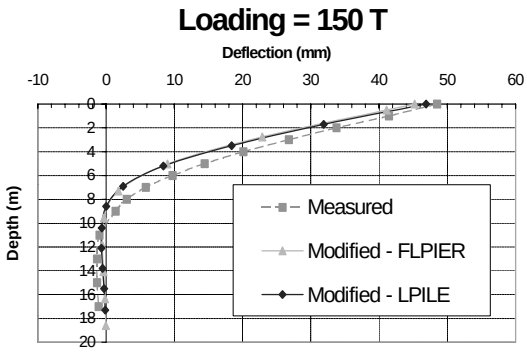

Figure A-13. Predictions of deflected shape of Bored Pile B2 using FLPIER and LPILE plus with modified p-y *criteria—load = 150 T (1.47 MN).*

from Pile B2 were not used in modeling the bored pile group, because a comparison of Figure A-9 for the slurry bored pile with Figure A-10 for the full depth–casing pile shows that, although there are local, depthwise differences in the *p-y* curve corrections, the mean correction is about equal for both methods of construction. This suggests that there was no advantage from the point of view of maintaining soil properties around the piles in using one construction method over the other.

On the other hand, a comparison of Figures A-9 (Bored Pile B1) and A-11 (Driven Pile P13) indicates that smaller modifications had to be made to the *p-y* curves for the driven piles than had to be made for the bored piles. The modifications that were made were generally to stiffen the *p-y* curves for the driven piles whereas the *p-y* curves had to be softened, in general, for the bored piles.

Two numerical models (i.e., computer codes) were used to analyze the single pile–test results: LPILE (*3*) and FLPIER (*15*). Both codes simulate nonlinear bending and axial load effects in laterally loaded concrete piles using similar procedures, and both use *p-y* curves to represent the soil in an identical manner. The results from both codes were essentially identical, as is demonstrated for Pile B2 in Figure A-13. However, FLPIER was selected for further use in this study because it was desired ultimately to develop *p*-multipliers that could be used in FLPIER.

The modified *p-y* curves shown in Figures A-9 through A-11 were accepted as the correct set of *p-y* curves for the test site for bored and driven piles, respectively, of the sizes used in the test groups. The *p-y* curves below a depth of 12 m were taken as the curves predicted by the standard *p-y* criteria. These curves were used without any site-specific modifications. Any deviations from these families of *p-y* curves that were needed to model the group tests were considered to be the results of (a) pile group construction, including installation order; and (b) pile-soil-pile interaction during lateral loading.

Pile Group Tests

Effects of Pile Construction on Soil Property Indexes

When the pile group construction was completed, but prior to load testing of the groups, soundings were made though small access holes in the pile caps to assess the index properties of the soil within the pile groups compared with index properties before the piles were installed. Several different types of probes were used. Two will be considered here: the seismic piezocone (SCPTU) and the DMT. Locations of the probes within each group are shown in Figures A-2 and A-3. Changes from initial values prior to construction to values obtained by probing the soil within the groups for q_c (i.e., cone-tip reading corrected for pore pressure) and E_d (i.e., the dilatometer modulus) are shown in Figures A-14 through A-17 for both the bored pile group and the driven pile group (*16*). The differences in initial and post-construction readings are denoted by the symbol "Δ" in those figures.

In comparing Figures A-14 and A-15, it is obvious that there was a tendency for q_c to decrease because of pile installation in the upper 12 m in the bored pile group; in the same depth range in the driven pile group, the tendency was for q_c to increase because of pile installation. Similarly, in comparing Figures A-16 and A-17, it is seen that the dilatometer modulus decreased within the bored pile group, while there was a slight tendency for it to increase in the driven pile group above a depth of 12 m. These data strongly suggest that the installation

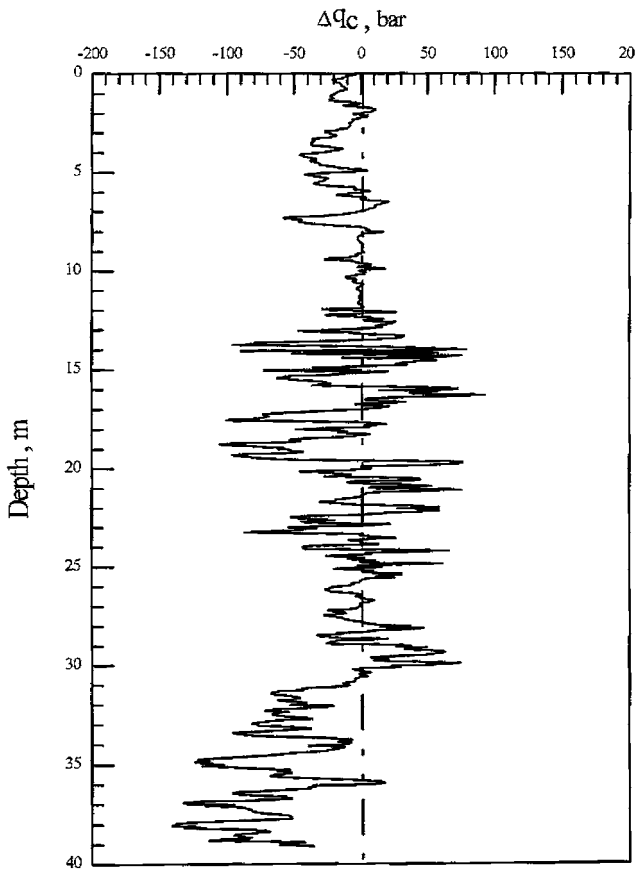

Figure A-14. Change in cone-tip reading (q_c) within bored pile group from preinstallation value to value obtained after piles installed (SCPTU-N1) (after Huang [16]).

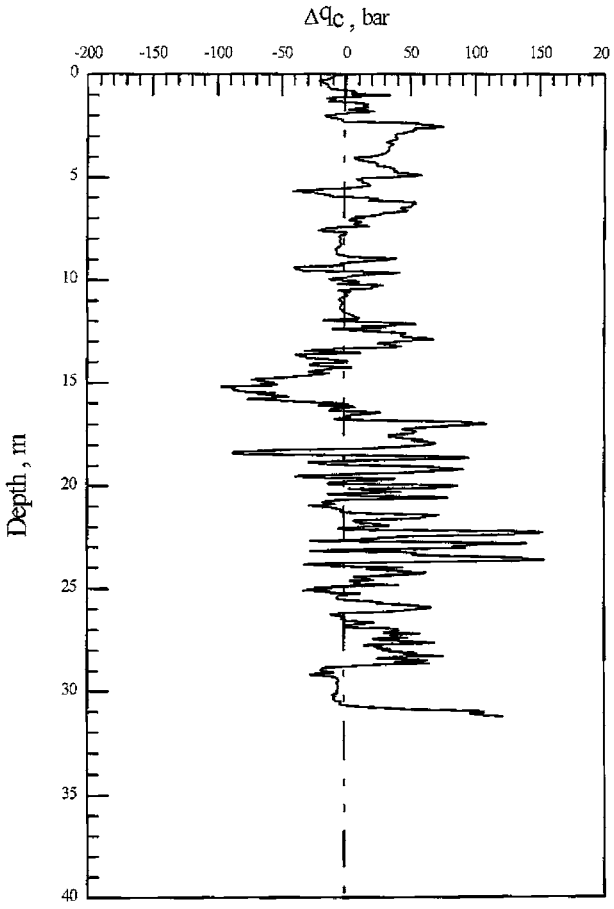

Figure A-15. Change in cone-tip reading (q_c) within driven pile group from preinstallation value to value obtained after piles installed (SCPTU-N3) (after Huang [16]).

of bored piles loosened the soil between the piles within the bored pile group or, perhaps, reduced lateral effective stresses, or both. On the other hand, the installation of the driven piles increased the soil density or lateral effective stresses, or both. These data suggest that the *p*-multipliers that are necessary to simulate group behavior using the site-specific (modified) single-pile *p-y* curves as a baseline will likely be different in the two groups.

Lateral Load Tests

The groups were tested approximately 2 months after the single reference piles were tested, using a quasi-monotonic loading procedure that was very similar to the procedure used for the single piles. The groups were loaded by essentially jacking them apart. The results of the load tests, in terms of cap translation versus lateral load (applied 0.5 m above the ground surface), are shown in Figures A-18 and A-19. A maximum load of 1000 tonnes (17.8 MN) was applied to each group. It is obvious that the bored pile group, consisting of six 1.5-m-diameter piles, was much stiffer than the driven pile group, consisting of twelve 0.8-m-diameter piles, despite the fact that the installation method seemed to weaken the soil around the bored piles within the group.

This seemingly anomalous behavior (from a soil-mechanics perspective) was likely caused by two important factors. First, the bored piles were tied into the pile cap through heavy, hooked rebars, with full development lengths extending into the pile cap, which were assumed to provide a moment connection between the pile cap and the pile heads. No such moment connection existed between the pile cap and the driven piles, in which the cast-in-place concrete for the steel-reinforced pile cap was merely poured over the extended heads of the driven piles. The driven group piles therefore behaved more as free- or pinned-headed piles than as fixed-headed piles. Moment connections stiffen the group response considerably, relative to pinned connections. Second, the sum of the moments of inertia of the 6 bored piles was higher than that of the 12 driven piles, which further stiffened the bored pile group. The fact that the bored pile group was stiffer despite the obvious disadvantages of using bored piles with regard to

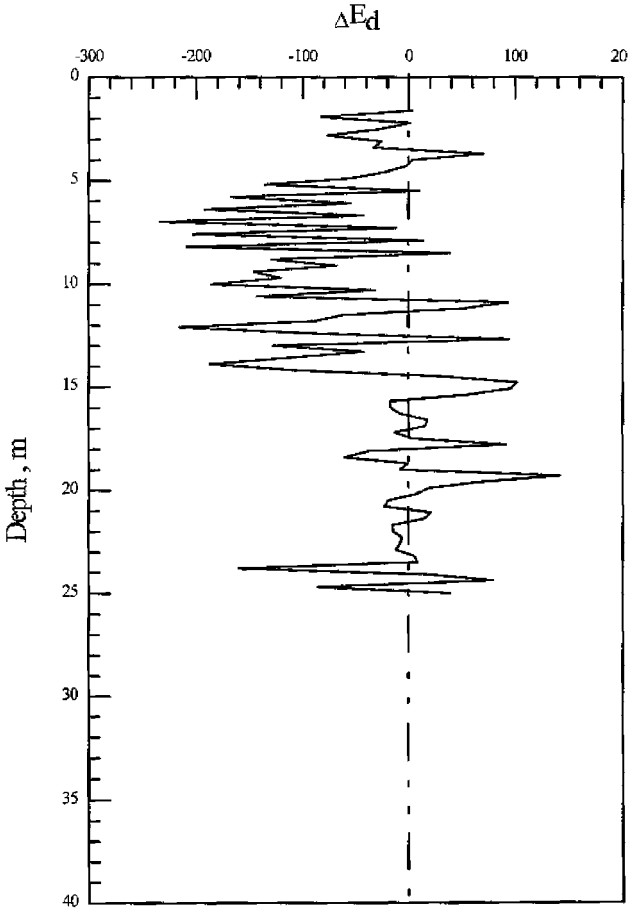

Figure A-16. Change in dilatometer modulus (E_d) within bored pile group from preinstallation value to value obtained after piles installed (DMT-N1) (after Huang [16]).

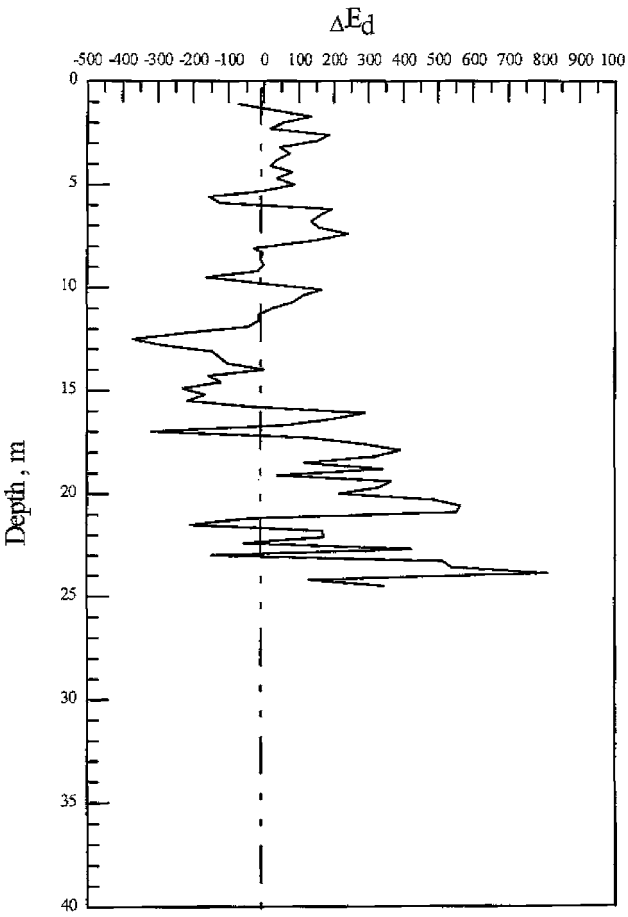

Figure A-17. Change in dilatometer modulus (E_d) within driven pile group from preinstallation value to value obtained after piles installed (DMT-N3) (after Huang [16]).

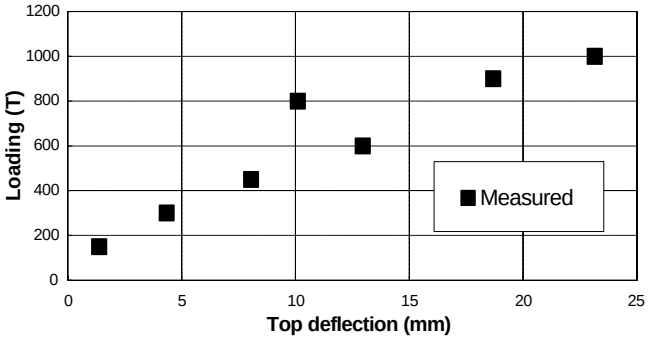

Figure A-18. Cap shear load versus lateral cap deflection—bored pile group.

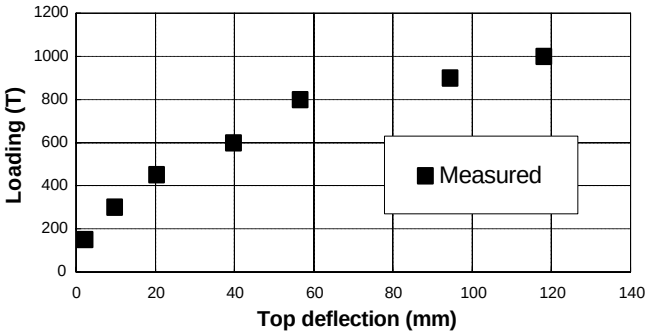

Figure A-19. Cap shear load versus lateral cap deflection—driven pile group.

the stiffness of the soil between the piles indicates the significance of the behavior of the structural components of the pile-soil-cap system and the importance of modeling correctly the structural performance of the pile group system.

On the other hand, a measure of the effects of soil softening caused by lateral pile group action in both groups is evident in Figures A-20 and A-21. The depths of significant lateral pile deflection are much deeper in these figures, from the group tests, than in the corresponding figures for the single-pile tests, Figures A-4 and A-5. The loads shown in Figures A-4 and A-5 are loads per pile whereas those shown in Figures A-20 and A-21 are loads for the entire group. Note that there is some discrepancy in measured head deflections among piles in Figure A-20. The lateral deflections at the head of each pile (at the base of pile cap) should be equal; hence, the differences in head deflections in Figures A-20 and A-21 are indications of the reliability of the deflection readings, which seemed to be comparable in both groups.

Modeling Group Behavior

Both group tests were modeled in a preliminary step using Program GROUP 4.0 (*17*) and FLPIER Version 5.1. Both codes gave similar results for the group load tests at small loads; however, it is necessary to model nonlinear bending in the piles at higher loads, which is not done automatically in GROUP 4.0. This nonlinearity made it difficult to account for the effects of the prestress on the bending stiffness of the driven piles at higher loads. The prestressing force is applied as a uniform axial load along the pile in FLPIER. This force retards the onset of tensile cracking and the resulting reduced bending stiffness in the piles. Eventually, however, the piles develop tensile cracks, which reduce bending stiffness. FLPIER handles this effect automatically. GROUP 4.0 gave a stiffer response than did FLPIER for the bored pile group at higher loads because GROUP 4.0 did not automatically adjust pile stiffness when cracking moments were applied. (In the cases of both bored and driven piles, bending stiffness can be reduced by the user in GROUP 4.0, making multiple runs when combinations of computed bending moments and axial loads indicate that there will be cracking in the cross section; however, this process is slow and inconvenient compared with using FLPIER, which makes the stiffness adjustments for flexural cracking automatically.) FLPIER also allows the user to model the bending flexibility of the pile cap whereas GROUP 4.0 assumes that the pile cap undergoes rigid body motion. Because the pile diameters in the bored pile group were large relative to the thickness of the cap, cap bending was a possibility, and the ability to simulate this phenomenon was a virtue in the group model. For these reasons, and because it

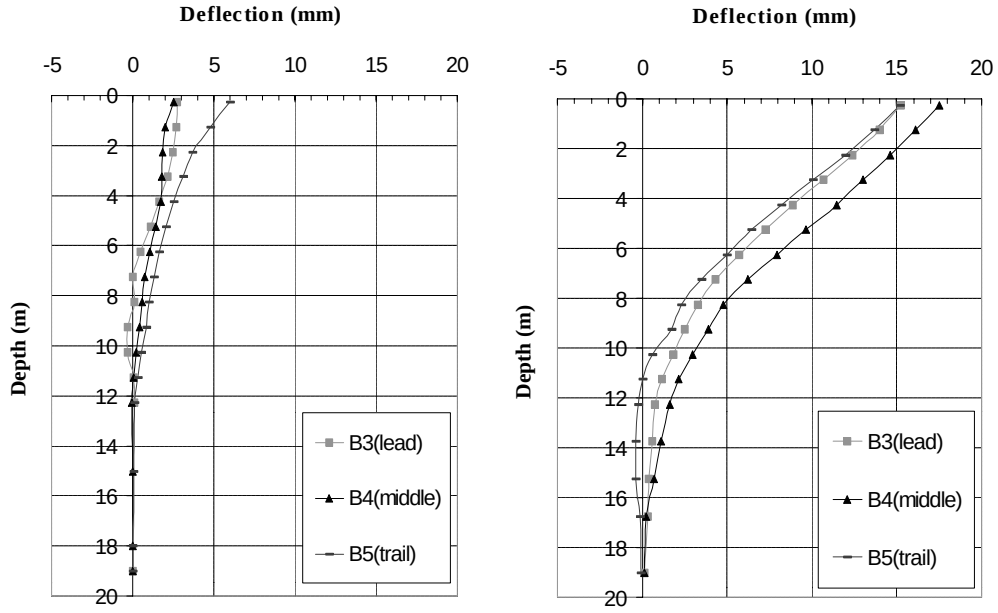

(a) Load = 300 T. *(b) Load = 800 T.*

Figure A-20. Measured deflected shapes along selected piles in bored pile group.

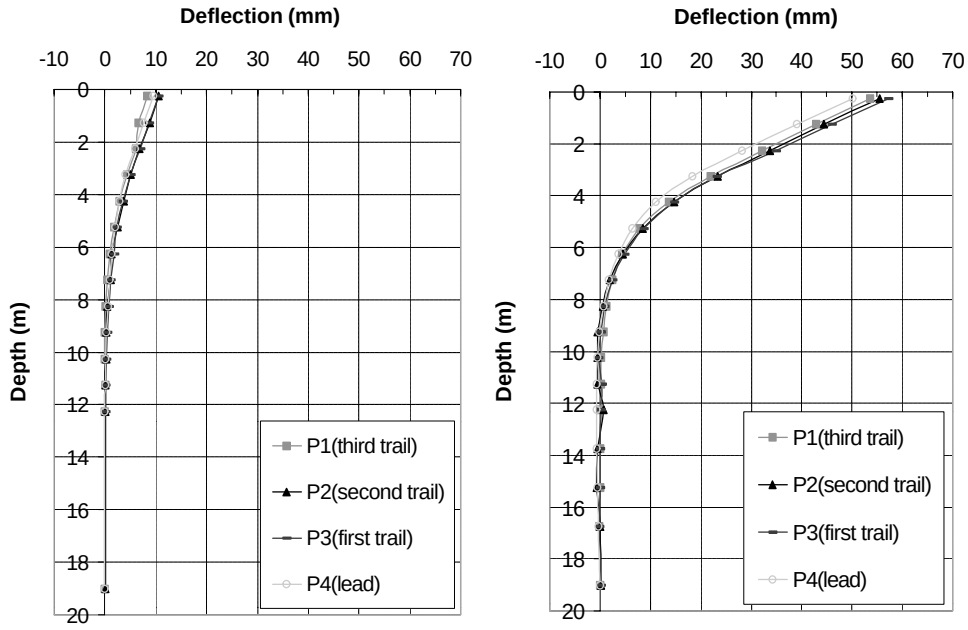

(a) Load = 300 T. *(b) Load = 800 T.*

Figure A-21. Measured deflected shapes along selected piles in driven pile group.

was desired to compute the *p*-multipliers directly for FLPIER, further work with GROUP 4.0 was abandoned.

The pile-head and group-cap conditions that were modeled by FLPIER are shown in Figures A-22 and A-23. All soil that had surrounded the bottom parts of the pile caps was removed physically prior to the tests so that there was no passive resistance or side shearing resistance against either cap. However, both caps were cast on the ground. No measurements of the shearing stresses between the bottoms of the caps and the soil were made, and no reliable measurements of shear load distribution among the piles were available. It was assumed, therefore, that the contribution of cap base shear to the total group

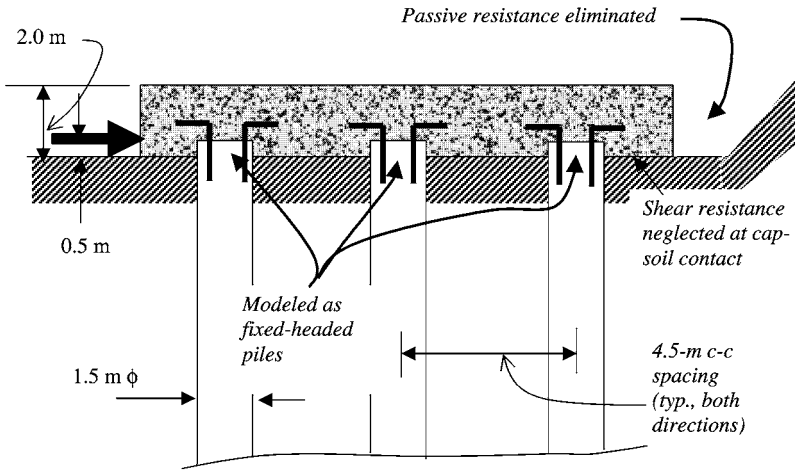

Figure A-22. FLPIER modeling for arrangement for bored pile group.

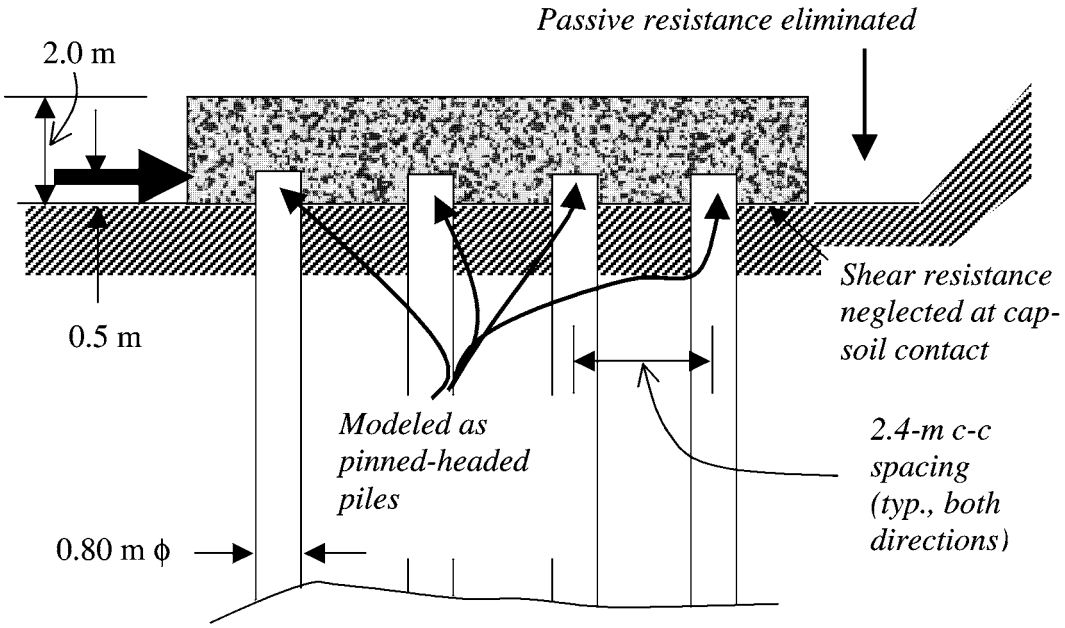

Figure A-23. FLPIER modeling arrangement for driven pile group.

resistance was very small, and it was neglected in the FLPIER analyses.

A less obvious, but no less important, phenomenon that had to be modeled with FLPIER in the simulation of the behavior of the fixed-headed bored pile group was the rotational stiffness of the group, or the axial "push–pull" couples that resist the applied moment (applied load times 0.5 m, as shown in Figures A-22 and A-23) and the "fixing" moments that are produced at the pile heads as the cap translates. These latter moments cause the cap to rotate and the fixing moments to relax, thus softening the lateral response of the pile group. The degree to which the cap rotates under loading from the fixing moments depends upon the stiffness of the group piles in the axial push–pull mode. It is therefore important to model the axial stiffnesses of the piles when the pile heads are assumed to be fixed into the pile cap because these stiffnesses directly influence the *p-y* curves that are required to be used to provide a match with the lateral deflection measurements.

Unfortunately, the only axial load test that was available for direct determination of unit axial load transfer curves for the bored piles, which can also be supplied to FLPIER to simulate axial pile stiffness, was the test on Pile B10. That pile, however, was installed using the full depth–casing technique, rather than the direct-slurry-displacement technique used in the group piles. Unit axial load transfer curves (sometimes called "*t-z*" and "*q-z*" curves), therefore, were generated using an internal routine in FLPIER, which uses an approximate method based on principles given by Randolph and Wroth (*18*). The axial stiffness calculations are carried out by using a simple discrete element model to which *t-z* and *q-z* springs are attached. In order to generate the *t-z* and *q-z* curves in FLPIER, it is only necessary to specify a value of soil shear modulus in the free field, *G*, and the ultimate value of unit side shear f_{max} and of base resistance q_{max}. *G* was estimated in the coarse-grained soil layers from Equations A-1 and A-2:

$$G = \frac{E}{2(1 + \nu)}, \tag{A-1}$$

where

E (force/length^2 in pounds per square foot [psf]) = 10,000 N_{60}. (A-2)

In Equation A-2, N_{60} is the standardized SPT blow count (the average value in a given layer). Poisson's ratio (ν) was taken to be 0.3. For fine-grained soil layers, Equation A-1 was used to estimate *G* whereas *E* was obtained from Equations A-3 and A-4:

$$G = \frac{50\, s_u}{(1 + \nu)}, \tag{A-3}$$

where

$$s_u(\text{in tsf}) = 15N_{60}. \tag{A-4}$$

In Equation A-4, s_u is the undrained shear strength of the fine-grained soil. Poisson's ratio (ν) was taken to be 0.5.

The ultimate unit side and base resistances were obtained from the American Petroleum Institute (API) (*19*), which are strictly valid only for driven piles but which were assumed to give appropriate values for bored piles, as well. In coarse-grained soils, f_{max} is set equal to $\sigma'_v K \tan\delta \le f_{max}$ (limit), where σ'_v is the vertical effective stress at the center of a given soil

layer; K is an earth pressure coefficient taken equal to 0.8; and δ is an angle of pile-soil wall friction prescribed by API Recommended Practice 2A (API RP2A) (*19*), based on the fines content and relative density of the soil. f_{max} (limit) is based on the same properties. q_{max} in compression is defined by σ'_v (base) N_q, where N_q is a function of fines content and relative density $\leq q_{max}$ (limit). q_{max} (limit) is likewise given by API to be a function of fines content and relative density and is set equal to zero for uplift loading.

In fine-grained soils, f_{max} is determined in API RP2A from the ratio of s_u to σ'_v. q_{max} is taken to be 9 s_u at the base of the pile for compression loading and zero for uplift loading.

Once the axial load–movement behavior of single piles was simulated in FLPIER, that value was used for each bored pile in the group without modification for axial group effects. The argument for making this simplifying assumption was that the front (i.e., leading) row of piles would settle, the back (i.e., trailing) row of piles would go into tension, and the middle row of piles would essentially remain stationary axially. The tendency for one pile on the front row to soften the behavior of its neighbor on that row is approximately offset by the tendency for the uplift in both piles in the back row to stiffen the behavior of the piles on the front row, with similar effects for piles on the back row.

No strong concern about modeling of axial behavior existed for the driven pile group because no fixing moments develop with pinned-headed piles, and the lateral stiffness is essentially decoupled from the axial push–pull behavior. Nonetheless, the same procedure was used for simulating axial response in the driven pile group as that used for the bored pile group.

With the modeling of axial behavior accomplished, the main effort in modeling the test groups with FLPIER was to determine how the site-modified, single-pile *p-y* curves (Figures A-9 and A-11) were required to be modified again to produce the *p-y* curves best suited to modeling group behavior. The second-step modification (for group action) was made by multiplying the site-modified *p-y* curves in Figures A-9 (for the bored piles) and A-11 (for the driven piles) by appropriate *p*-multipliers specific to each row of piles, from the leading row to the last trailing row.

The concept of the *p*-multiplier, as applied in this study, is briefly explained in Figure A-24. For each pile on a given row in the group (leading, first-trailing, second-trailing, and so forth), all of the *p*-values on all of the *p-y* curves at every depth are multiplied by a single factor, ρ (i.e., the *p*-multiplier for that row in the group). ρ was varied in the FLPIER model until an acceptable match was found between the computed and measured load-deformation behavior of the pile cap for both group tests. By following the procedure outlined in this appendix, the factor ρ describes the combined effect of group construction and group loading on lateral pile group action.

The ρ values (i.e., *p*-multipliers) were ascertained by varying ρ on a row-by-row basis and comparing the computed cap translations at seven values of cap load, ranging from 150 T (1.47 MN) to 1000 T (9.8 MN). The number of loads at which the absolute value of the computed deflection minus the measured deflection divided by the measured value of deflection exceeded 15 percent was considered a measure of the accuracy of the selected family of ρ values. The results of a subset of analyses of the effects of families of ρ values on cap displacement in the bored pile group are summarized in Table A-2. The most accurate family of ρ values for the bored pile group is shown in Column 8 of Table A-2 although the families of values in Columns 2 and 10 are essentially of equal accuracy.

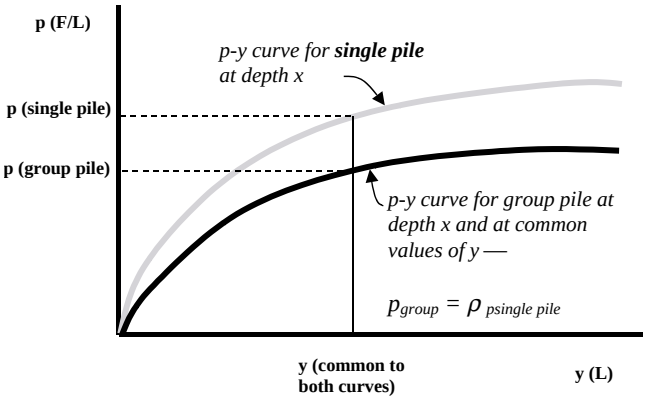

Figure A-24. Definition of the p*-multiplier (*ρ*) for simulating lateral group behavior.*

The optimum set of ρ values (i.e., *p*-multipliers) for each group is presented in Table A-3. Also shown in Table A-3 are values that have been cited by Peterson and Rollins (*8*) as being appropriate for laterally loaded pile groups based on information available in 1996. The *p*-multipliers for the bored pile group in the current study were, on the average, lower than those cited by Peterson and Rollins; the *p*-multipliers for the driven pile group were higher, row by row and on the average, than those of Peterson and Rollins. Considering the independent soil data of Huang (*16*) in Figures A-14 through A-17, these trends appear to be clearly related to installation methods.

The measured lateral load versus lateral-translation relations for both pile groups are compared with the relations predicted by FLPIER using the site-specific (modified) *p-y* curves for both bored and driven piles (see Figures A-9 and A-11, respectively). The *p*-multipliers tabulated in Table A-3 are shown in Figure A-25. The predictions are excellent.

Finally, a typical comparison of computed and measured deflected shapes for group piles is shown in Figure A-26. The FLPIER model with the modified *p-y* curves and the deduced *p*-multipliers appears to give good predictions of pile shape under loading. Further details on the field tests and the analysis of the field tests can be found in Reference 20 (*20*).

CONCLUSIONS AND RECOMMENDATIONS

Conclusions

Although the knowledge obtained from the Chaiyi field tests and their analysis is site specific, the general conclusions stated below are expected to be valid for other sites at which similar

TABLE A-2 Effect of varying *p*-multipliers on cap deflection for the bored pile group

Load (T)	Measured cap deflection (mm)	Computed cap deflection (mm) (1)	(2)	(3)	(4)	(5)	(6)	(7)	(8)	(9)	(10)	(11)	(12)
		0.8	0.6	0.6	0.6	0.7	0.7	0.5	**0.5**	0.5	0.5	0.65	0.55
		0.4	0.3	0.3	0.2	0.2	0.3	0.3	**0.4**	0.4	0.3	0.35	0.47
		0.333	0.3	0.2	0.3	0.3	0.2	0.3	**0.3**	0.2	0.4	0.2	0.13
150	1.38	1.81	2.15	2.32	2.31	2.19	2.20	2.28	**2.14**	2.31	2.13	2.18	2.26
		+31%	+55%	+68%	+67%	+59%	+59%	+65%	**+55%**	+67%	+54%	+58%	+64%
300	4.34	3.48	4.17	4.58	4.56	4.24	4.27	4.57	**4.22**	4.61	4.20	4.24	4.51
		-20%	-4%	+6%	+5%	-2%	-2%	+5%	**-3%**	+6%	-3%	-2%	+4%
450	8.05	6.09	7.55	8.21	8.17	7.62	7.65	8.06	**7.49**	8.19	7.43	7.65	7.95
		-24%	-6%	+2%	+2%	-5%	-5%	+0%	**-7%**	+2%	-8%	-5%	-1%
600	12.96	7.85	9.8	10.8	10.8	10.0	10.0	10.6	9.7	10.7	9.67	10.0	10.4
		-39%	-24%	-17%	-17%	-23%	-23%	-18%	-25%	-17%	-25%	-23%	-20%
800	10.1	11.8	15.3	17.0	17.0	15.6	15.7	16.7	**15.2**	16.9	15.2	15.5	16.4
		+17%	+52%	+68%	+68%	+55%	+55%	+65%	**+50%**	+67%	+50%	+55%	+62%
900	18.69	14.6	19.1	21.5	21.5	19.5	19.5	21.1	**18.9**	21.3	18.9	19.3	20.5
		-22%	+2%	+15%	+15%	+4%	+4%	+13%	**+1%**	+14%	+1%	+3%	+10%
1000	23.15	19.5	26.6	30.1	30.1	27.2	27.2	29.6	**26.4**	29.9	26.4	27.0	29
		-16%	+15%	+30%	+30%	+18%	+18%	+28%	**+14%**	+29%	+14%	+17%	+25%
Average difference ratio		-10%	+13%	+25%	+24%	+15%	+15%	+23%	**+12%**	+24%	+12%	+15%	+21%
Error probability		7/7	3/7	4/7	4/7	4/7	4/7	4/7	**3/7**	4/7	3/7	4/7	4/7

NOTE: The percentage below each computed deflection is the ratio of the difference between a computed and measured deflection to the measured deflection; "Average difference ratio" is the value of the sum of all the difference ratios in a column divided by the number of total loads (i.e., 7); "Error probability" is defined as the ratio of the number of the loads whose corresponding difference ratios exceed ±15% to the number of total loads.

soil conditions exist (loose to medium-dense silty sands and sandy silts near the surface) and at which piles are installed with a similar geometry (rectangular groups with 3-diameter, center-to-center pile spacing) by casting the piles in place or by driving displacement piles. Please note that these conclusions cannot be extended to sites at which liquefaction will occur, nor is it likely that these conclusions apply to predominantly clay sites. The conclusions can be stated as follows:

1. Single-pile *p-y* curves needed to be softer (i.e., reduced *p*-values for given values of *y*) than the prescribed curves (i.e., Reese et al. [*1*] criteria for sand layers; Matlock [*13*] criteria for clay layers) for large-diameter (1.5-m) bored piles. See Figure A-9.
2. Single-pile *p-y* curves did not require overall softening relative to the prescribed curves (i.e., Reese et al. [*1*] criteria for sand layers; Matlock [*13*] criteria for clay layers) for smaller-diameter (0.80-m) driven displacement piles; however, some modification—both softening and stiffening—at individual depths was needed to optimize the simulation of measured single-pile behavior. See Figure A-11.
3. The ratio of the deduced *p*-multipliers for the quasi-static loading of bored piles, averaged over all rows, was

TABLE A-3 *p*-Multipliers for Chaiyi lateral group load tests

Pile Row	Inferred *p*-Multipliers from Chaiyi Load Tests: Bored Pile Group	Inferred *p*-Multipliers from Chaiyi Load Tests: Driven Pile Group	*p*-Multipliers from Peterson and Rollins (*8*) *S / D* = 3	Default *p*-Multipliers from FLPIER (*15*) *S / D* = 3
Lead	0.5	0.9	0.6	0.8
First Trail	0.4	0.7	0.4	0.4
Second Trail	0.3	0.5	0.4	0.2
Third Trail	–	0.4	–	0.3
Average	*0.4*	*0.63*	*0.47*	*0.43*

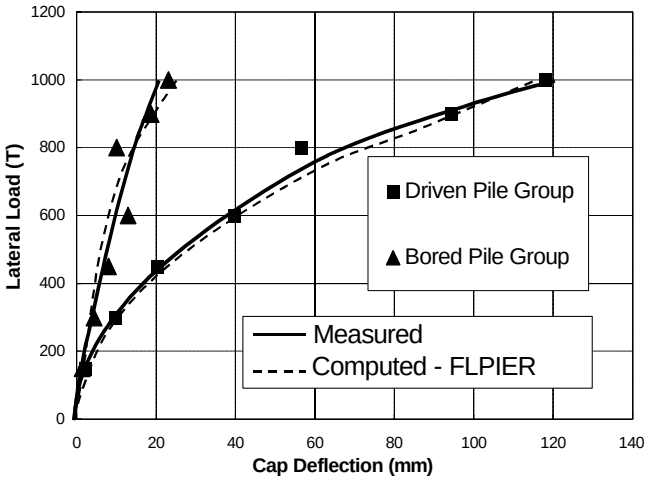

Figure A-25. Measured lateral load-cap deflection relationships for driven and bored pile groups.

approximately 0.65 times that for the quasi-static loading of driven displacement piles. The ratio of the average *p*-multiplier for the bored piles to the average "standard" value recommended by Peterson and Rollins (*8*) was 0.85; the ratio of the average *p*-multiplier for the driven displacement piles was 1.33 times the value recommended by Peterson and Rollins. See Table A-3.

4. The row-wise pattern of *p*-multipliers for both the driven and bored pile groups, tabulated in Table A-3, was similar to that observed by others. That is, the highest values appeared on the leading (i.e., front) row, the next highest on the first trailing row, and so forth. (When the extreme-event loading has a predictable direction, it is appropriate to use row-wise *p*-multipliers in the design process. In seismic events, however, loading direction likely varies, and loading is cyclic, making it more reasonable from a design perspective to use average *p*-multipliers for all piles in the group.) The exact row-to-row ratios of *p*-multipliers is likely a function of the order of pile installation. In this study, the installation order was generally from front (i.e., leading) row to back (i.e., last trailing) row.
5. Apparently, the differences in *p*-multipliers for bored and driven piles largely reflect the effects of the differing effects of boring and driving displacement piles on the density and stress state in the mass of soil within the pile group.
6. The reduced soil stiffness around the bored piles was overshadowed by the effects of head fixity and pile diameter (i.e., the higher moment of inertia) in the bored pile group.

The applicability of the results summarized in this appendix to *p*-multipliers for dynamic loading (see Appendix B) is not clear. However, the results suggest that for low frequencies of seismic loading (low predominant frequency of the seismic event), the average *p*-multiplier for groups of bored piles should be lower than those for driven displacement piles by a factor in the range of 0.65.

Recommendations for Further Research

The following additional research is recommended:

1. Further research is needed to understand the frequency range to which the ratio of *p*-multipliers for bored piles to those for driven piles, deduced from static tests such as these tests, applies.
2. It is possible that *p*-multipliers will be different for bored piles installed with continuous, full-depth casing

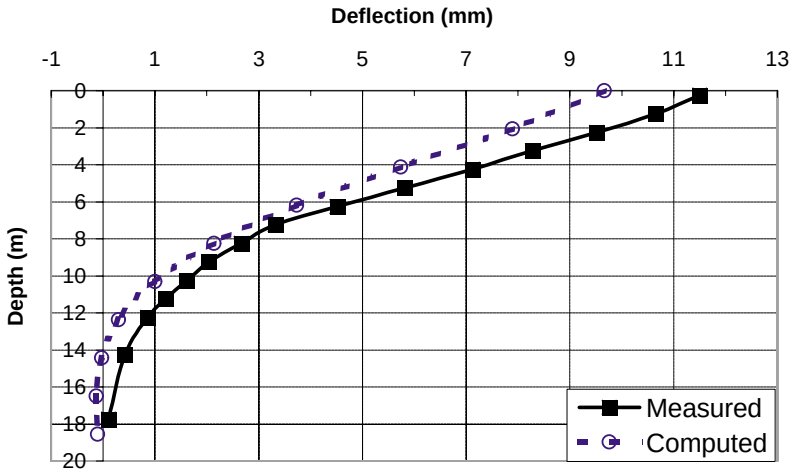

Figure A-26. Measured and predicted deformed shape of Pile B3 on leading row of the bored pile group—load = 600 T.

than for bored piles installed by slurry displacement. Further research into this phenomenon is warranted if full depth–casing construction methods become common on department of transportation projects in the United States.

REFERENCES—APPENDIX A

1. Reese, L. C., W. R. Cox, and F. C. Koop. "Analysis of Laterally Loaded Piles in Sand," *Proceedings, Offshore Technology Conference*, Houston (1974); pp. 473–484.
2. Murchison, J., and M. W. O'Neill. "Evaluation of p-y Relationships in Cohesionless Soil," *Analysis and Design of Pile Foundations*, J. R. Meyer (ed.); ASCE (1984); pp. 174–191.
3. Reese, L. C., and S. T. Wang. *Computer Program LPILE Plus, Version 3.0—A Program for the Analysis of Piles and Drilled Shafts Under Lateral Loads, Technical Manual.* Ensoft, Inc. (1997).
4. Hoit, M., C. Hays, and M. McVay. "The Florida Pier Analysis Program: Methods and Models for Pier Analysis and Design," *Transportation Research Record No. 1569*, Transportation Research Board, National Research Council (1997); pp. 1–7.
5. *PAR: Pile Analysis Routines, Theoretical and User's Manuals.* PMB Engineering, Inc. (1988).
6. Brown, D. A., C. Morrison, and L. C. Reese. "Lateral Load Behavior of Pile Group in Sand," *Journal of Geotechnical Engineering*, ASCE, Vol. 114, No. 11 (1988); pp. 1326–1343.
7. McVay, M., R. Casper, and T.-I. Shang. "Lateral Response of Three-Row Groups in Loose to Dense Sands at 3D and 5D Pile Spacing," *Journal of Geotechnical Engineering*, ASCE, Vol. 121, No. 5 (1995); pp. 436–441.
8. Peterson, K., and K. M. Rollins. *Static and Dynamic Lateral Load Testing of a Full-Scale Pile Group in Clay*, Research Report CEG.96-02. Brigham Young University (1996).
9. Pinto, P., M. McVay, M. Hoit, and P. Lai. "Centrifuge Testing of Plumb and Battered Pile Groups in Sand," *Transportation Research Record No. 1569.* Transportation Research Board, National Research Council (1997); pp. 8–16.
10. Brown, D. A., and C. F. Shie. "Modification of p-y Curves to Account for Group Effects on Laterally Loaded Piles," *Geotechnical Special Publication No. 27*, ASCE, Vol. 2 (1991); pp. 479–490.
11. Chen, C.-H. "Data for Planned Pile Group Tests at Chaiyi Test Site," *Workshop Report.* National Taiwan University (1996).
12. Huang, A. B. *Midterm Report of the Lateral Test of Group Piles.* National Chao-Tung University (Taiwan) (1997).
13. Matlock, H. "Correlations for Design of Laterally Loaded Piles in Soft Clays," *Proceedings, Second Annual Offshore Technology Conference*, Houston, (1970); pp. 578–588.
14. Andrade, P. *Materially and Geometrically Nonlinear Analysis of Laterally Loaded Piles Using a Discrete Element Technique, Final Report.* University of Florida (1994).
15. McVay, M., C. Hays, and M. Hoit. *User's Manual for Florida Pier, Version 5.1.* University of Florida (1996).
16. Huang, A. B. *The Effect of the Installation of Group Piles on the Properties of the Soil in the Vicinity, Final Report.* National Chao-Tung University (Taiwan) (1997).
17. Reese, L. C., and S. T. Wang. *GROUP 4.0 for Windows: Technical Manual.* Ensoft, Inc. (1996).
18. Randolph, M. F., and C. P. Wroth. "Analysis of Deformation of Vertically Loaded Piles," *Journal of the Geotechnical Engineering Division*, ASCE, Vol. 104, No. GT12 (1978); pp. 1465–1488.
19. *Recommended Practice for Planning, Designing and Constructing Fixed Offshore Platforms—API Recommended Practice 2A* (RP2A), 17th Edition. American Petroleum Institute (1993).
20. Zhang, X. "Comparison of Lateral Group Effect between Bored and PC Driven Pile Groups in Sand," M.S. thesis. Department of Civil and Environmental Engineering, University of Houston (1999).